

Neuroimaging of headaches attributed to cranial and/or cervical vascular disorders

Gerta Repeckaite¹, Agne Smigelskyte¹, Rymante Gleizniene²

¹Lithuanian University of Health Sciences, Academy of Medicine, Faculty of Medicine, Kaunas, Lithuania

²Lithuanian University of Health Sciences, Academy of Medicine, Faculty of Medicine, Clinic of Radiology, Kaunas, Lithuania

ABSTRACT

Secondary headaches comprise approximately 10% of all headache cases. They often have a serious underlying condition that needs prompt and thorough examination, which almost always includes neuroimaging. Each imaging modality serves a different purpose, and various diagnostic methods can be utilized in the diagnostics of headaches attributed to cranial and cerebral vascular disorders which vary in both etiology and manifestation. This literature review aims to summarise and present the role of neuroimaging in the evaluation of patients with the conditions above.

Keywords: neuroimaging; headache disorders, secondary; radiology

INTRODUCTION

Headache is a recurrent or persistent pain of the head (1). It has a lifelong prevalence of 66-96% and the current prevalence of 46% (1, 2) and is a common presenting complaint in the emergency department, responsible for approximately 2% of all visits (3). Headaches are divided into primary (with no underlying cause) and secondary (caused by another condition) (4). Primary headaches are more common – they comprise 90% of all cases (5). Although rare, secondary headaches are often life-threatening and require immediate action (6). However, diagnosis more often than not requires imaging evaluation of the head. This article aims to present different aspects of secondary headaches attributed to cranial or cervical vascular disorders with a particular focus on neuroimaging of the underlying condition.

REVIEW OF LITERATURE

Headache attributed to a cerebral ischemic event Ischemic stroke is an episode of neurological dysfunction which lasts more than 24 hours and is caused by focal cerebral, spinal or retinal infarction (7). It is a common neurological disorder with an incidence ranging from 95 to 290 per 100 000 inhabitants in Europe (8). Observational studies indicate that 8%–64% of patients report a

headache at the onset of an acute ischemic stroke (9). Generally, the stroke associated headache is not severe but continuous and manifests as bilateral tension-type head pain. (10). Basilar strokes are associated with headaches more often than carotid strokes while lacunar strokes are generally not accompanied by headaches at all (9). A small number of migraine patients infrequently suffer from migrainous strokes with an incidence of 0,8 per 100 000 inhabitants (11).

Headache at stroke onset is predictive of a headache development at six months post-stroke (12). Persistent headaches attributed to past ischemic events have been estimated to occur in 10% of post-stroke patients. A post-stroke headache is predominantly characterized as a tension-type headache with a pressing quality (13).

In the setting of an acute stroke, neuroimaging is performed to exclude possible hemorrhages, to assess the degree of brain injury, and to identify the vascular lesion responsible for the ischemic deficit (14).

Non-contrast computed tomography (CT) scans are the first modality of choice in case of acute ischemic stroke because of their wide availability and rapidity of imaging (15). Non-contrast CT scans are useful in detecting large ischemic strokes after 6 to 8 hours from onset. Non-contrast CT has an overall sensitivity of 57-71% to detect an acute ischemic stroke in the first 24

hours but only 12% in the first 3 hours (16, 17). Early non-contrast CT findings include hypoattenuation in the territory of the middle cerebral artery, hypodensity of the lentiform nucleus, cortical sulcal effacement, focal parenchymal hypoattenuation, loss of the insular ribbon or obscuration of the Sylvian fissure, hyperattenuation of large vessels, loss of gray and white matter differentiation in the basal ganglia (14).

Alberta Stroke Program Early CT Score (ASPECTS) method assists in evaluating early ischemic changes in CT scans. ASPECTS is a scoring system of 10 points and can be applied only to the territory of the middle cerebral artery (18, 19).

CT angiography (CTA) provides the means to rapidly and noninvasively evaluate the intracranial and extracranial vasculature in stroke patients, thus providing valuable information about the presence of vessel occlusion or stenosis (20). CTA has a sensitivity of 92-100% and specificity of 82-100% for the detection of intracranial large vessel occlusion and stenosis (21). A noninvasive intracranial vascular study is a must before endovascular therapy (15, 20).

Magnetic Resonance Imaging (MRI) is superior to CT in detecting hyperacute stroke (14). Fluid attenuation inversion recovery (FLAIR) and T2 weighted (T2W) sequences become positive within the first 3 to 8 hours after an acute arterial occlusion. The MRI signs of acute ischemic stroke include increased brain signal intensity, swollen cortical gyri, and increased signal intensity in the lumen of vessels (16). Diffusion-weighted imaging (DWI) is a form of MRI that is capable of detecting brain tissue damage during the first 3 to 30 minutes of ischemia, making it the most sensitive early neuroimaging technique in the setting of an acute ischemic stroke (Figure 1) (23).

A transient ischemic attack is a temporary episode (less than 24 hours in duration) of neurological dysfunction caused by focal brain, spinal, or retinal ischemia without any evidence of acute infarction (7). Headache is rarely a prominent symptom of a transient ischemic attack – its frequency varies between 16 and 36% (24). In the case of transient ischemic attack, head CT or MRI must be performed to exclude infarction.

DWI can be used to distinguishing brain, spinal, or retinal ischemia from an acute infarction (25).

HEADACHE ATTRIBUTED TO NON-TRAUMATIC INTRACRANIAL HEMORRHAGE

Headache attributed to non-traumatic intracerebral hemorrhage (ICH)

Intracerebral hemorrhage (ICH) is defined as haemorrhage into the brain parenchyma and occurs with the incidence of approximately 25 cases for every 100 000 inhabitants annually (26). Non-traumatic or spontaneous ICH is caused by a variety of aetiologies, the most common reasons being hypertensive or amyloid angiopathy (27). Headache is one of the most prevalent symptoms of ICH (28). The manifestation of the headache does not depend on the cause and is usually gradual (29); however, it may also manifest as a thunderclap headache (30). Other common symptoms include nausea, vomiting, focal neurological deficit symptoms, deteriorating consciousness, etc. (31).

Since clinical presentation is not sufficient for the differentiation between ischemic and hemorrhagic focal neurological symptom origins, imaging modalities are imperative. The gold standard for acute hemorrhage detection is non-contrast CT or gradient recalled echo (GE) and T2*-susceptibility-weighted MRI (31, 32). CT scan findings assist with clinical decisions by evaluating hematoma volume and predicting the upcoming 30-day mortality (34). Contrast-enhanced CT and CTA may be useful in assessing the risk of hematoma expansion by detecting focal areas of contrast within the hematoma (known as the spot sign) (35–37) or a large number of cerebral microbleeds (38).

In the setting of ICH, CT is inferior to other imaging modalities, such as MRI and angiography, especially sometime after the onset. Nonetheless, as mentioned previously in this review, in emergency diagnostics, CT is the preferred imaging modality for its availability, cost-effectiveness, and rapidity. CT angiography/venography (CTA/CTV), and contrast-enhanced MRI or MR angiography/venography (MRA/MRV) are informative when there is suspicion of an underlying structural lesion (39). Detected hyperin-

tense lesions in DWI indicate acute or subacute ICH (Figure 2) (40). MRI and MRA are far more sensitive when diagnosing older hemorrhages, secondary (primarily structural) causes, such as arteriovenous malformations, tumors, and cerebral venous thrombosis (27, 31, 32, 40).

Headache attributed to non-traumatic subarachnoid hemorrhage (SAH)

1% of all emergency room visitors suffering from headaches are diagnosed with subarachnoid hemorrhage (SAH) (3). SAH is defined as hemorrhaging into the cerebrospinal fluid (CSF) due to corticomeningeal vessel rupture and occurs in approximately 8 out of 100 000 people per year (42). Multiple underlying conditions may be responsible for the development of SAH: various vascular disorders, traumas, blood dyscrasias, etc. (43) Common SAH manifestations include a sudden severe thunderclap headache which can be the only manifestation of the condition (43, 44). Additional symptoms involve changes in consciousness, neurological deficits, seizures, vomiting, and neck stiffness (46). Due to its high prevalence, neuroimaging in the setting of SAH is a widely researched topic. However, currently, there is a significant disparity in opinions concerning the diagnostic protocols (47).

The most common clinical practice is to perform a non-contrast CT scan, followed by lumbar puncture (LP) if the head CT scan is non-diagnostic (48). This protocol is still considered to have the highest sensitivity, while MRI/MRA and CT/CTA are alternative imaging modality protocols, useful in cases where CT/LP is contraindicated or hazardous (49). Furthermore, CT has lower sensitivity when diagnosing SAH in the posterior fossa, in patients without focal neurological abnormalities, and cases of small hemorrhaging volumes (50). Current data suggest that MRI FLAIR sequence is more sensitive than or equal to CT when detecting acute or subacute SAH (42, 50–52) and additional scanning protocols may be useful when diagnosing an underlying condition (54). Nonetheless, negative MRI would still require a follow-up LP (55).

LP is an invasive procedure, which prompts an effort to find a similar or even more sensitive diagnostic tool. It has been hypothesized that CTA could replace LP in the SAH diagnostics

as a non-invasive and thus safer procedure with relatively high sensitivity (42). However, data from the recent studies suggest that it would not be an optimal approach seeing as asymptomatic aneurysms could be unnecessarily diagnosed and the imaging modality comes with unwarranted radiation exposure as well as considerable expenses (41, 55, 56). On the other hand, modern third-generation cranial CT scans performed within the first 6 hours of headache onset and evaluated by a qualified radiologist have incredibly high specificity and sensitivity (100% each), which warrants the elimination of a follow-up tool altogether (58–60). This suggests that improved CT scanning protocols negate LP necessity and dangers, which occur due to having a higher probability of complications than of diagnosis (61–63). However, the 6-hour CT diagnostic sensitivity applies only to the patients that have no focal neurological abnormalities or changes in consciousness (64) and CT sensitivity drops to 50% at seven days. Meanwhile, LP is diagnostic from 12 hours post-ictus and up to two weeks after the onset (65).

Once a diagnosis has been established, further imaging modalities are required to determine the cause.

HEADACHE ATTRIBUTED TO NON-TRAUMATIC ACUTE SUBDURAL HEMORRHAGE (ASDH)

Acute subdural hemorrhage (ASDH) is defined as acute bleeding between the dura and arachnoid membranes usually due to damage to the bridging veins (66). Spontaneous ASDH is less common than traumatic subdural hemorrhages, however, it is more dangerous due to higher mortality (67). Non-traumatic ASDH may be caused by multiple conditions, such as impaired hemostasis, cerebral aneurysms, ruptured cortical artery, arteriovenous malformations, neoplasms, hypertensive cerebral hemorrhage, intracranial hypotension, Cerebral Amyloid Angiopathy (CAA), and acquired immune deficiency syndrome (68). The headache manifests suddenly in accordance with the site of hemorrhaging and peaks in seconds or minutes, typically just before the focal neurological symptoms (30).

Non-contrast CT is integral in both initial clinical decision making and as a follow up (67). The

main feature of ASDH as seen on a CT scan is usually a hyperdense and sometimes mixed appearance of the subdural space (69). MRI is more sensitive when diagnosing extremely thin, hemispheric or tentorial subdural hemorrhages (70). Imaging parameters, evaluated in the setting of ASDH are age or thickness of the hemorrhage, midline shift, presence of blood in the basal cisterns, ventricle obstruction. Additionally, underlying conditions may be visualized using CT, MRI, CTA, MRA and other imaging modalities (66). For example, vascular imaging of the head is advisable in patients with spontaneous ASDH without coagulopathy, due to the possibility of a ruptured cranial aneurysm (71–76).

Persistent headache following non-traumatic ICH, SAH, ASDH

Headaches that persist more than three months after a non-traumatic intracranial hemorrhage have no specific imaging characteristics and thus are not described in this review.

HEADACHE ATTRIBUTED TO UNRUPTURED VASCULAR MALFORMATION

HEADACHE ATTRIBUTED TO UNRUPTURED SACULAR ANEURYSM

An unruptured intracranial saccular aneurysm is a protrusion from a cerebral artery that consists of a damaged or absent tunica media and an internal elastic lamina (77). It occurs in 1–2% of the population (78). Sometimes unruptured intracranial aneurysms manifest as a thunderclap headache, loss of visual acuity or palsy of the 3rd cranial nerve but usually, they are asymptomatic (64, 77). Therefore, an unruptured aneurysm is often an incidental radiological finding. Aneurysms of 3 mm or larger can be identified on CT (79), but CTA is frequently required to clarify the diagnosis. CTA has specificity rates of 96–98% (90–94% for aneurysms smaller than 3 mm and up to 100% for aneurysms larger than 4 mm) and sensitivity rates of 96–98% for the detection of an intracranial unruptured saccular aneurysm (79, 80). The majority of saccular aneurysms are found around the anterior and posterior communicating arteries, the bifurcation of the middle cerebral artery, the internal carotid artery, the basilar artery, the superior cerebellar

artery and the posterior inferior cerebellar artery (64, 76). Just like CT, MRI has a somewhat limited role in detecting an unruptured saccular aneurysm. However, three-dimensional time-of-flight MRA with volume rendering at 3.0 Tesla has a sensitivity of 99% and specificity of 97% which is irrespective of aneurysm size (81, 82). Digital subtraction angiography is indicated in the case of negative CTA/MRA or before surgical or endovascular treatment to evaluate adjacent structures and blood flow patterns (Figure 3) (84).

HEADACHE ATTRIBUTED TO ARTERIOVENOUS MALFORMATION

Arteriovenous malformation (AVM) is a congenital disorder of the brain or spinal cord characterized by an abnormal tangle of arteries and veins with varying amounts of fistulas (85). Brain AVMs have a prevalence of 18 per 100 000 inhabitants (86). Presenting symptoms of AVM are intracranial bleeding, headache, seizures, and focal neurological deficits (85). Signs of AVM on non-contrast CT include a usually hyperdense nidus with enlarged draining veins in the periphery of the brain parenchyma. CTA may improve the sensitivity of CT to identify brain AVMs. (87). Signs of AVM on MRI include the nidus, feeding arteries, and draining veins that demonstrate flow void and can be seen on conventional sequences (65), while MRA may help confirm the more subtle AVMs (Figure 4) (88). The diagnosis of AVM is confirmed by cerebral angiography (87).

HEADACHE ATTRIBUTED TO DURAL ARTERIOVENOUS FISTULA

Dural arteriovenous fistula (DAVF) is an abnormal connection between meningeal arteries and dural venous sinuses or subarachnoid veins (89). It has a detection rate of 0.16–0.29 per 100 000 inhabitants each year (90). DAVF frequently presents as painful pulsatile tinnitus or a headache with other symptoms of intracranial hypertension (91). A diagnostic evaluation usually starts with head non-contrast CT or MRI (92). CTA and MRA characterize the feeding arteries, early dural sinus opacification, and prominent draining veins (89). The diagnosis is confirmed with digital subtraction angiography which remains

the gold standard in the case of DAVFs (64, 93). Headache attributed to cavernous angioma
Cavernous angioma occurs in 0.4 – 0.8% of the population and is described as a vascular malformation of the brain and spinal cord characterized by a lack of tight junctions between the lining endothelial cells of pathologically dilated blood vessels and slow blood flow within the pathological structure (94). Some cavernous angiomas may trigger cluster headache-like, SUNCT-like (short-lasting unilateral neuralgiform headache with conjunctival injection and tearing) or migraine-like attacks. The location of the headache typically coincides with the site of the cavernous angioma (30). The primary imaging modality for cavernous angiomas is MRI. The most common finding is a reticulated lesion with mixed signal intensities (Figure 5) (95).

HEADACHE ATTRIBUTED TO ENCEPHALOTRIGEMINAL OR LEPTOMENINGEAL ANGIOMATOSIS (STURGE-WEBER SYNDROME)

Encephalotrigeminal or leptomeningeal angiomatosis (Sturge-Weber syndrome) is a congenital vascular disorder characterized by a capillary or capillary-venous malformation of the face, brain, and eye (96). It occurs in approximately 1 in every 20 000 – 50 000 newborns (97). Encephalotrigeminal or leptomeningeal angiomatosis may cause migraine attacks with long motor auras (30). Other symptoms include port wine stain on the face, seizures, hemiparesis, visual disorders, behavioral problems, and mental retardation (98). The primary neuroimaging technique for the diagnosis of this disorder is brain MRI with gadolinium contrast (96). Pia and cortical enhancement are usual signs of Sturge-Weber syndrome on MRI (99). CT is less useful but may detect brain calcification and atrophy (98). Angiography can reveal the lack of superficial cortical veins and tortuous veins near the vein of Galen (98). Positron Emission Tomography (PET) or Single Photon Emission Computed Tomography (SPECT) are rarely used in diagnosing Sturge-Weber syndrome, but abnormal glucose metabolism and cerebral perfusion may be detected before the presence of clinical symptoms (Figure 6) (98).

HEADACHE ATTRIBUTED TO ARTERITIS

The current gold standard for diagnosing various forms of arteritis is a vessel biopsy. However, neuroimaging plays a major role in screening and with increasing improvements may rival the sensitivity and specificity even of the aforementioned invasive procedure.

HEADACHE ATTRIBUTED TO GIANT CELL ARTERITIS

Giant cell arteritis (GCA) is a granulomatous vasculitis of medium and large arteries (100). This idiopathic and chronic condition occurs in people older than 50 years with an incidence ranging from 6,9 to 32,4 per 100 000 inhabitants (101). Headache is a presenting symptom in two-thirds of GCA patients, but it has no specific characteristics apart from the occasional complaint of scalp tenderness to touch (102). Other symptoms of GCA include fever, fatigue, weight loss, jaw claudication, and vision loss (103).

Temporal artery biopsy is the gold standard for establishing the diagnosis of GCA. However, it might not be necessary in case of typical symptoms and specific ultrasound or MRI findings (104). Colour duplex ultrasonography of the temporal arteries remains an important and widely available imaging modality of GCA. The halo sign (dark, hypoechoic circumferential wall thickening) is highly sensitive and specific to GCA (102). Meanwhile, MRI and MRA enable the evaluation of vessel wall inflammation. The sensitivity and specificity of MRI for GCA ranges from 68% to 89% and from 73% to 97% respectively (104). MRA can detect an irregular outline and diameter changes of the arteries wall (101). In cases of GCA, CT is useful when diagnosing concentric mural thickening which continues over long segments and indicates vessel inflammation, while CT angiography is more suitable in the assessment of stenotic and aneurysmal lesions of arteries that develop as complications (105). Further detection of inflammatory changes in the blood vessels can be achieved through 18F-FDG-PET (often combined with CT) based on the uptake of the radioligand. However, in comparison to MRI, this diagnostic method has lower sensitivity and specificity (77% and 66% accordingly) (106, 108).

HEADACHE ATTRIBUTED TO PRIMARY OR SECONDARY ANGIITIS OF THE CENTRAL NERVOUS SYSTEM (PACNS AND SACNS)

Angiitis of the central nervous system (CNS) refers to a broad spectrum of diseases that result in inflammation and destruction of arteries and veins of the brain, spinal cord, and meninges. Inflammation typically causes medium or small brain blood vessels to become narrowed, occluded, and thrombosed, which results in brain tissue ischemia and necrosis (17). Angiitis of the CNS could be either primary (confined to the CNS) or secondary (part of a multisystem inflammatory disease) (107). PANCS is a rare disease with an incidence of 2.4 per 1 million inhabitants (108). Headache is the dominant symptom of both primary and secondary types of angiitis. Typically it is subacute, insidious, and diffuse but may present in a variety of other characteristics. However, a thunderclap headache should raise suspicion of a reversible cerebral vasoconstriction syndrome which often mimics PACNS (109). Other symptoms of angiitis of the CNS include cognitive impairment, focal deficits, seizures, cranial nerve involvement, myelopathy, and ataxia. Weight loss, fever, or the involvement of visceral organs are usually signs of systemic vasculitis (110). Conventional cerebral angiography is often considered to be the radiological gold standard for the diagnosis of PACNS/SACNS. The typical angiographic finding is defined as beading (alternating areas of stenosis and dilatation) (110). However, some studies have shown that the sensitivity and specificity of cerebral angiography for PACNS might be as low as 70% and 30% respectively (109).

In comparison, MRI has a high sensitivity of 90-100% for diagnosing PACNS but a low specificity. Most common MRI findings, occurring in approximately 53% of patients, are multifocal brain infarcts, while parenchymal hemorrhage, leptomeningeal and parenchymal enhancement are observed less frequently (110, 113, 114). MRA and CTA are less sensitive for angiitis of the CNS than conventional cerebral angiography or MRI. They are useful in evaluating large brain vessels, but angiitis of the CNS typically involves medium and small vessels (107). Brain tissue bi-

opsy of radiographically involved areas remains the gold standard for establishing the diagnosis of PACNS (113).

HEADACHE ATTRIBUTED TO CERVICAL CAROTID OR VERTEBRAL ARTERY DISORDERS

Headache or facial or neck pain associated to cervical carotid or vertebral artery dissection

Cervical artery dissection (CAD) is a tear of the carotid or the vertebral artery wall resulting in the formation of a false lumen and intramural hematoma (114). It has an incidence of 2.6-5 per 100 000 inhabitants per year (8, 117). CAD accounts for 10% to 25% of ischemic strokes in young adults and some cases may also cause a subarachnoid hemorrhage (116). The expanding intramural hematoma of CAD may lead to local compression of adjacent nerves causing pain, lower cranial neuropathies or cervical nerve root damage (116, 119). Headache (with or without the pain of the neck) is the most common and sometimes the only manifestation of CAD occurring in 55-100% of cases (30). Pain is often unilateral (ipsilateral to the dissected artery), sudden, severe, prolonged (up to 3 months after the stabilization of CAD), and associated with Horner's syndrome, tinnitus or palsy of the 12th cranial nerve (30). In rare cases, the headache may not resolve within three months after the stabilization of CAD and become persistent (30). On the whole, the diagnosis of CAD is based on the detection of loss of integrity of the carotid or the vertebral artery wall. Ultrasound may visualize the lumen, the wall of the artery and the surrounding tissue. The most common findings of ultrasound in the case of CAD include an intramural hematoma, an echogenic intimal flap, floating thrombus within the vascular lumen, and tapering of the arterial lumen (117, 120). Doppler sonography reveals a bidirectional high resistance flow, reduced blood flow velocity or absence of flow, and no flow in the false lumen (119). The sensitivity of ultrasound for CAD is approximately 70% – 86%. Thus other neuroimaging modalities such as MRI/MRA or CTA are needed to establish the diagnosis (45, 122). MRI provides information about the occurrence of intramural hematoma, and MRA evaluates the

vascular lumen (116). The sensitivity and specificity of MRA and CTA for CAD are relatively similar (119, 123). However, CTA is used more often due to its wide availability and fast scanning speed (122). Conventional angiography for CAD is performed only in questionable cases due to its invasiveness and inability to evaluate the arterial wall. Usual signs of conventional angiography of CAD include vessel stenosis or occlusion, false or double lumen, pseudoaneurysm, irregular dilatation and, intimal flap (118). Conventional angiography used to be the gold standard for CAD, but nowadays it is replaced by MRA and CTA due to its high accuracy and wide availability (122).

POST-ENDARTERECTOMY HEADACHE

Carotid endarterectomy is a neurosurgical procedure performed to remove the atherosclerotic plaque from the inside of an artery and reestablish the diameter of the vessel lumen to prevent strokes (125, 126). There are three different types of headaches associated with carotid endarterectomy. The first type of pain is the most common. It occurs within the first few days after surgery as a diffuse and mild headache. The second type resembles a cluster headache occurring once or twice a day for roughly two weeks. The third type of headache is unilateral, pulsating and severe (30). It usually begins three days after surgery due to the hyperperfusion syndrome which is marked by an increase of cerebral blood flow, seizures, focal neurological deficits and may cause cerebral hemorrhage (125). Hyperperfusion can be detected via transcranial doppler which directly measures blood flow velocity of the middle cerebral artery (126). MRI and CT findings are indirect and include white matter edema, cerebral infarction, or hemorrhage, while perfusion-weighted MRI and single-photon-emission CT may directly indicate an increased cerebral blood flow (129, 130).

HEADACHE ATTRIBUTED TO THE CAROTID OR VERTEBRAL ANGIOPLASTY OR STENTING

Angioplasty or stenting of the carotid or the vertebral arteries is endovascular procedures performed to treat cervical artery stenosis and decrease the risk of stroke (129). Headache and

sometimes pain of the neck occur in one-third of patients and has a mild, ipsilateral, and pressing quality. Pain begins within one week and resolves within one month after the endovascular procedure (30). The cause of headache associated with angioplasty or stenting of the carotid or the vertebral arteries is the hyperperfusion syndrome which has already been described in the previous section (126, 131). Imaging modalities are utilized only when there is suspicion of other conditions or complications of the procedure.

Headache attributed to cranial venous disorder Cerebral venous thrombosis (CVT) is a potentially lethal condition and is most common in adults (with a mean age of 39 years), more so in women than in men (130). The incidence of this condition is 1.3 per 100 000 adults and maybe even higher in developing countries (131). A severe slow-onset diffuse headache is a common manifestation, occurring in more than 90% of cases, and usually accompanied by focal neurological symptoms that are a sign of a brain parenchymal lesion, and/or seizures that occur in 40% of all CVT cases (132, 134). Rarely the headache presents unilaterally, suddenly, thunder-likely, or mildly, not unlike a migraine (30).

Although CVT is a rather rare condition, early diagnosis and treatment, which are heavily dependent on the knowledge of neuroimaging methods and signs, are crucial (133). As usual, the primary imaging modality in the emergency department is non-contrast CT, which is often insufficient for diagnosis. However, increased attenuation of the obstructed cortical vein ("cord sign"), dural or the posterior portion of the superior sagittal sinus ("dense triangle sign") is indicative of CVT (136, 137). Additionally, Hounsfield unit (HU) to hematocrit ratio measurement has been suggested as a rather sensitive diagnostic criterion for CVT. However, further studies are required (136). In contrast-enhanced CT CVT manifests as the "empty delta sign": a contrast-enhanced wall of the thrombosed posterior superior sagittal sinus (137). Further indirect signs of CVT can be observed in CT scans: dilation of the venous structures, small ventricles, brain parenchymal lesions, falx and tentorium enhancement (138). Unfortunately, neither contrast-enhanced nor non-contrast negative

CT scans can rule out CVT.

In cases of CVT, MRI and MRV are the preferred modalities in all stages (133). MRV and CTV are both adequate for assessing changes in the venous system. However, CTV is inferior for the visualization of changes in the brain parenchyma (136, 141, 142). CTV is superior to Time-of-Flight MRV when diagnosing partial vessel occlusion (141). MRV as a separate imaging modality is not sufficient. CVT diagnosis requires a full MRI in addition to MRV (141, 144). The signal intensity of the thrombus depends on its age (139), and specific sequences have their advantages: susceptibility weighted or T2*W GE sequences are most beneficial when evaluating the obstruction in an acute setting or of the cortical vein (143). Contrast-enhanced MRV is superior to Time-of-Flight MRV for assessing smaller sinuses or slow blood flow (144). All in all, neither MRI nor CT is sufficient, and CTV or MRV are necessary when clinical suspicion of CVT is high (Figure 7). Catheter angiography is considered to be the most accurate diagnostic tool; however, due to its invasive nature, this method is rarely applied in clinical practice (135, 147).

Another reason for headaches, related to the cranial venous sinuses, is stenting. It is the most common adverse effect of the procedure, which occurs ipsilaterally to the stent and lasts for a few days. The precise frequency is difficult to determine due to many other stent unrelated types of headaches that patients experience following the procedure (146). The aforementioned adverse reaction to the cranial venous sinus stenting needs to be differentiated from other conditions, such as complications or comorbidities. However, neuroimaging has no different role to play in the diagnosis of this type of headache.

HEADACHE ATTRIBUTED TO OTHER ACUTE INTRACRANIAL ARTERIAL DISORDER

INTRACRANIAL ENDARTERIAL PROCEDURE RELATED HEADACHE AND ANGIOGRAPHY HEADACHE

Headaches associated to intracranial end-arterial procedures (IEP) include angioplasty, embolization, stenting, and typically develop within

the first week and resolve within a month, while headaches attributed to angiography develop within a day and resolve in 72 hours after the procedure (30). Typically, they are different in types of severity and duration; symptoms may be migraine-like in patients with an underlying migraine. IEP related headaches are typically unilateral (30). However, head imaging is required only when there is suspicion of complications, such as stent thrombosis or stroke.

Headache attributed to RCVS

Reversible cerebral vasoconstriction syndromes (RCVS) are known as a group of conditions that clinically manifest during physical exertion, sexual activity, Valsalva maneuvers, bathing, or emotional stress as a thunderclap headache due to a reversible multifocal dilation and constriction of the cerebral arteries (29, 149). Although the precise incidence is not known, it is believed that the condition is relatively common (112). RCVS is considered the most common cause of thunderclap headache in patients without an aneurysmal subarachnoidal hemorrhage, and the most common recurrent thunderclap headache (148). The thunderclap headache can be accompanied by nausea, photosensitivity, and focal deficits (151, 152). Additionally, a small percentage of RCVS patients report atypical headaches (151, 152). RCVS can lead to various types of intracranial hemorrhages (convexal subarachnoid, intracerebral, subdural hemorrhages), as well as posterior reversible encephalopathy syndrome (PRES) and ischemic stroke (151).

The prevention of the complications above requires early diagnosis and management of the RCVS (152–154). Imaging is an indispensable part of the diagnostic workup. However, various means of evaluation can be utilized: angiography, transcranial Doppler sonography, CT or MR angiography. More than a third of initial CT/MRI scans are normal in the presence of cerebral vasoconstriction (114, 151, 152). Nonetheless, imaging evaluation should begin with non-contrast CT. Convex subarachnoid hemorrhage especially in patients younger than 60 years of age, signs of previous and/or current multifocal infarcts, and typical clinical findings should raise suspicion of RCVS (157, 158). Further assessment requires CT angiography, MR angiography or conven-

tional angiography. CT angiography is less sensitive than conventional angiography; however, it is the setting of proximal branch involvement, CTA detects the segments of vasoconstriction in addition to possible comorbidities or complications (157).

MRI is superior to CT when evaluating possible complications and alternative diagnoses, yet remains insufficient for the diagnosis of RCVS (151, 152, 159). Hyperintense vessels along cerebral sulci in T2 FLAIR imaging, while not specific, are indicative of RCVS and higher risk of ischemic stroke and PRES incidence (152, 160, 161). Although MRA is less sensitive than conventional angiography, it is often utilized because of the non-invasive nature (155). MRA is used to assess the extent, distribution, and progression of the arterial constriction and associated complications (160). Even transcranial ultrasound has been utilized. However, this modality cannot exclude the diagnosis or RCVS (161).

Conventional cerebral angiography, although invasive, is considered to be the gold standard (151, 157). It has the superior spatial resolution to MRA and CTA and enables the assessment of small and distal cerebral arteries, which is why MRA and CTA sensitivity for RCVS-related arterial stenoses is 80% in comparison to conventional angiography (162, 164). Typical angiography findings in RCVS are segments of arterial constriction and dilatation, known as 'string of beads' or 'sausage on a string' signs (162).

Certain conditions, especially primary angiitis of the CNS, may manifest similarly to RCVS. Imaging plays a critical role in differentiation (155). Vessel Wall Imaging is an MR technique, useful when differentiating vasculitis from RCVS among other things. RCVS related wall thickening is less often enhanced, unlike in the setting of central nervous system vasculitis (165, 166). Perfusion imaging enables the detection of multifocal hypoperfusion areas, which helps with the evaluation of progression and treatment response in addition to the effects of specific segment stenosis (167, 168).

Persistent RCVS related headaches are longer than three months and persist even after the cerebral arteries normalize (30).

Headache attributed to intracranial artery

dissection

Intracranial artery dissection (IAD) is best known for its association with severe subarachnoid hemorrhages that tend to recur (169, 170). Headaches attributed to IAD present unilaterally and suddenly and may progress as subarachnoid hemorrhage or stroke (29, 171). The precise incidence is not known, however, it is believed to be less than 2.6 - 3.0 per 100 000 people (170).

Clinical presentation is not specific, and imaging evaluation is not always conclusive. Typical radiological signs include mural hematoma, intimal flap, and a double lumen (170). It is important to note that no modality can detect all of these findings, seeing as CT and MRI visualize the extraluminal, while CT/MR/conventional angiography detects intraluminal changes. In the setting of IAD, a mural hematoma is associated with enlarged external diameter, which is not related to other conditions that can manifest as intramural hematomas as well (170). 2 - 3 days following the onset of the IAD, MRI T1W sequence and exceptionally high-resolution 3 Tesla MRI that includes three-dimensional fat-suppressed T1W images with a black-blood effect can detect the hyperintense hematoma (171). An intimal flap is best observed in digital subtraction angiography (170). Dissection may also be accompanied by aneurysmal dilatation, which indicates a higher risk of subarachnoid hemorrhage, while segmental stenosis and occlusion in subarachnoid haemorrhage is indicative of IAD (172, 174, 175). CTA and MRA are useful when diagnosing intraluminal changes, while digital subtraction angiography is utilized only in cases of negative CT/MRI, before surgical or endovascular treatment, and when patients present with subarachnoid hemorrhage (170). Depending on the findings, a combination of CT/MRI and intraluminal imaging is often required to confirm the diagnosis of IAD.

HEADACHE ATTRIBUTED TO GENETIC VASCULOPATHY

HEADACHE ATTRIBUTED TO CADASIL
Cerebral Autosomal Dominant Arteriopathy with Subcortical Infarcts and Leukoencephalopathy (CADASIL) is a small vessel disease de-

terminated by a mutation in the NOTCH3 gene (174). It is considered to be the most frequent of all small vessel diseases and hereditary stroke disorders with a prevalence of approximately 2-5 cases per 100 000 inhabitants (11, 176–179). It manifests by the late middle age most frequently as a migraine with prolonged aura (29, 180). Additional symptoms include transient ischemic attacks and strokes, cognitive impairment, changes in mood and gait, epilepsy, and others (179). Neuroimaging plays a significant role in the diagnosis of CADASIL, even in patients presenting with no symptoms whatsoever (180). Typically, CADASIL is differentiated from other small vessel diseases by detecting early subcortical ischemic changes that progress to involve the anterior temporal poles and less frequently the external capsule or the superior frontal gyrus (182, 183). MRI T2W and FLAIR sequences show the extent and age of the white matter abnormalities that typically progress with years, while the DW sequence enables the quantification of chronic white matter changes (184, 185). Other less prevalent pathological MRI findings, common to CADASIL are CSF filled lacunas, cortical infarctions, and involvement of corpus callosum (182, 185, 186).

Other imaging modalities are less sensitive when detecting changes, common to CADASIL. In the preliminary stages of the disease, CT imaging may reveal nonspecific periventricular white matter hypodensities. However, the common anterior temporal lobe abnormalities can be diagnosed only in the advanced stages of CADASIL (181). Therefore, CT may indicate the disease. However, MRI is necessary to confirm the diagnosis (Figure 8). Few studies analyze the diagnostic value of FDG-PET and diffusion tensor imaging. However, even those studies suggest that findings are not specific to CADASIL (181).

Headache attributed to MELAS

Mitochondrial Encephalopathy, Lactic Acidosis and Stroke-like episodes (MELAS) are known as one of the maternally inherited mitochondrial metabolic diseases that often manifest before the fourth decade of life as a multisystemic disorder (186). Certain features of MELAS overlap with CADASIL, but the main symptoms include migraine-like attacks, stroke-like episodes, and

encephalopathy often with dementia and/or seizures (187).

The clinical manifestation of MELAS is intricate. Nonetheless, brain imaging visualizes white and grey matter changes that are characteristic and aid the diagnosis of MELAS. In patients, presenting with stroke-like symptoms, infarction simulating lesions are unlike the vascular territories, develop slowly, may change location, and progress into atrophic regions with time (189, 190). Typically, the involvement of parietal and occipital lobes is observed (189). While MRI findings are similar to CADASIL (both conditions are known for the subcortical white matter damage), cortical area involvement with vasogenic edema and mass effect in acute and subacute phases is more indicative of MELAS (190). Seeing as typical radiological findings are brain parenchymal lesions, MRI is the preferred modality (189, 192). Common CT scan findings include bilateral basal ganglia and thalamic calcifications (192). DWI is useful when differentiating cytotoxic from vasogenic edema, the latter usually but not always manifesting in MELAS as elevated ADC and sometimes progressing to cytotoxic (193–198). SPECT findings differ between studies and depend on the acuity of MELAS (198, 200–202). CTA, MRA, and catheter angiography may be utilized to evaluate the obstruction of cerebral arteries and in MELAS; it is common to find the arteries of the seemingly ischemic zones to be patent (201). Other imaging modalities, such as PET, Arterial Spin Labeling, Oxygen Extraction Fraction, Magnetoencephalography, and transcranial ultrasound may be utilized when there are doubts concerning the diagnosis (202–206).

HEADACHE ATTRIBUTED TO MMA

Moyamoya angiopathy (MMA) is described as a chronic progressive disease, defined by an abnormal vasculature at the base of a brain following bilateral stenosis and/or occlusion of the terminal inferior cerebral artery branches (207). This disease is most prevalent in Asia, with 10.4 cases per 100 000 patients in Japan (208). MMA is yet another condition, associated with recurring and migraine-like headaches, which may manifest as a stroke in early childhood or adolescence (30). Neuroimaging enables the confirmation of the

diagnosis. Head CT scan visualizes infraction of both cortical and subcortical areas or parenchymal hemorrhages into the basal ganglia, thalamus, ventricles, however, it does not provide information on the vasculature itself (209–211). MRI is more sensitive than CT when diagnosing MMA and enables the detection of findings that suggest MMA even in asymptomatic cases. Characteristic findings indicative to MMA are the dilatation of leptomenigeal and cortical collateral vessels (known as the “ivy sign”), absent flow voids in the distal portions of inferior and middle cerebral arteries, and absent signal in the basal ganglia (212–216). High-resolution MRI further increases the sensitivity of this modality, by visualizing the narrowing of the outer arterial wall diameter, and long-segment concentric enhancement of the inferior or middle cerebral artery. These findings raise the suspicion of MMA even in the early stages (217–220). Other, MMA common findings observed on MRI are ischemic lesions in deep watershed zones (221), and asymptomatic cerebral microbleeds (223, 224). Noninvasive or catheter angiography is required for the detection of steno-occlusion of the inferior, middle, and/or anterior cerebral artery, and grading, according to Suzuki’s six stages (224). Conventional angiography is performed usually in cases when bypass surgery is being considered (212). Additional studies may be utilized for the evaluation of intracranial hemodynamics: transcranial sonography, perfusion CT, MRI, PET, SPECT, arterial spin labeling, etc. (225–230).

HEADACHE ATTRIBUTED TO CAA

Cerebral Amyloid Angiopathy (CAA) is a small and medium-sized vessel disease that affects the walls of the leptomeninges and cerebral cortex vessels due to the accumulation of amyloid- β (231). The prevalence of the disease increases with age and dementia development: autopsy results observed CAA related changes in up to 60% of dementia patients and 28-38% of nondementia patients (232). Patients suffer from late-onset auras, typically without or with a mild headache as well as other typical CAA dementia symptoms (30).

Although definite diagnosis requires validation by pathological brain tissue examination, neuro-

imaging can detect findings indicative of CAA (233). Lobar hemorrhages, commonly in the temporal and occipital regions, usually visualized by T2*W GE MRI sequences, raise suspicions of CAA in dementia patients (234, 235). Although CAA may be the reason for ICH, it has been concluded that the vast majority of CAA patients do not suffer ICH (235).

In patients over 60, CAA is considered to be the most common cause of convex subarachnoidal hemorrhage (156), which in turn increases the risk of future ICH (236). Another finding, common to small vessel disease, is cerebral microbleeds, which are seen as small hypointense areas on blood-sensitive T2*W GE or susceptibility-weighted MRI sequences (237). Cerebral microbleeds correlate with microvascular leakage and are not specific to any condition. However, lobar cerebral microbleeds are indicative of CAA and increased intracerebral hemorrhage and ischemic stroke risks (237–242). White matter hyperintensity (leukoaraiosis) is a specific diagnostic term, which is used to describe low-density areas on CT scans and high signal areas on T2W MRI scans. It has been hypothesized that particular localization (occipital region) of leukoaraiosis may indicate CAA, even though white matter hyperintensity is common in most small vessel disease (243).

Meanwhile, cortical superficial siderosis is identified by specific MRI sequences and occurs more often in CAA patients than in the general population (Figure 9) (245, 246). In addition, cortical superficial siderosis indicates a high risk of recurrent ICH (246). Finally, PET assessment of amyloid deposit localization has diagnostic value and may predict the occurrence of CAA related ICH (247).

HEADACHE ATTRIBUTED TO RVCLSM

Retinal vasculopathy with cerebral leukoencephalopathy and systemic manifestations (RVCLSM) is a hereditary neurovascular syndrome caused by mutations in the TREX1 gene (248). This condition is best known for retinal vasculopathy, brain dysfunction, in addition to white matter and intracerebral mass lesions on neuroimaging, while systemic manifestations are less frequent (248). The headache is defined as mi-

graine-like episodes, often without aura, with or without other clinical features (30).

The diagnosis is based on genetic testing, while characteristic neuroimaging manifestations occur and progress from the fifth decade (249). CT is not sufficient as the disease affects mostly the white matter of the brain and merely focal calcifications can be observed (248). MRI is superior and can detect punctate non-enhancing T2-hyperintense lesions in the periventricular and subcortical white matter, or enhanced punctate lesions either with DWI related restriction or with various rim enhancements (more familiar to the later stages) that are generally associated with edema and mass effect (248). Typical enhanced lesions as seen on an MRI are considered to be the major diagnostic criteria, while the aforementioned non-enhanced MRI and focal calcifications on CT are minor criteria of the RVCLSM (248).

HEADACHE ATTRIBUTED TO OTHER CHRONIC INTRACRANIAL VASCULOPATHY

In theory, all intracranial vasculopathy can cause migraine-like attacks. However, this group includes migraine-like headaches with and without aura by any chronic vasculopathy (30). There are no specific neuroimaging indications or findings. Thus the imaging evaluation of these headaches is not discussed in this review.

HEADACHE ATTRIBUTED TO PITUITARY APOPLEXY

Pituitary apoplexy (PA) is a potentially life-threatening clinical syndrome that is characterized by the sudden enlargement of the pituitary gland frequently following infarction of a preexisting pituitary adenoma (250). It is a rare condition with an estimated 6.2 cases per 100 000 inhabitants (251). PA often manifests as a sudden and severe thunderclap headache, commonly accompanied by visual disturbances, diplopia, changes in consciousness, less frequently nausea, vomiting, and hypotension (253, 254).

Imaging plays a crucial role in the diagnosis of PA. It helps to rule out other conditions, such as subarachnoidal hemorrhage, meningitis, cerebral sinus thrombosis, midbrain infarction, migraine, and aneurysms (250). The measurement

of the pituitary mass influences clinical decisions (252). Due to the sudden onset of the condition, the first diagnostic test is usually a non-contrast CT of the head. However, in cases of a negative CT, patients should undergo an MRI scan, seeing as MRI is far more accurate when diagnosing subacute PA (253, 255–257). Two signs of PA can be observed on a CT scan: an interstellar mass (80% of cases) and hemorrhagic components (20–30% of cases) (253, 258). In contrast-enhanced CT certain features of the pituitary tumor may become visible: inhomogeneous enhancement with or without ring enhancement (258). It has been reported that MRI findings are sensitive enough to be comparable to histopathological conclusions (259). T1W sequences are useful for detecting altered signal intensity sella turcica lesions, while T2W images detect hemorrhages (260). T2*W GE imaging increases the sensitivity of blood product detection even further (261). All in all, imaging, especially MRI, plays a crucial role in diagnosis and decision making in the setting of PA (Figure 10).

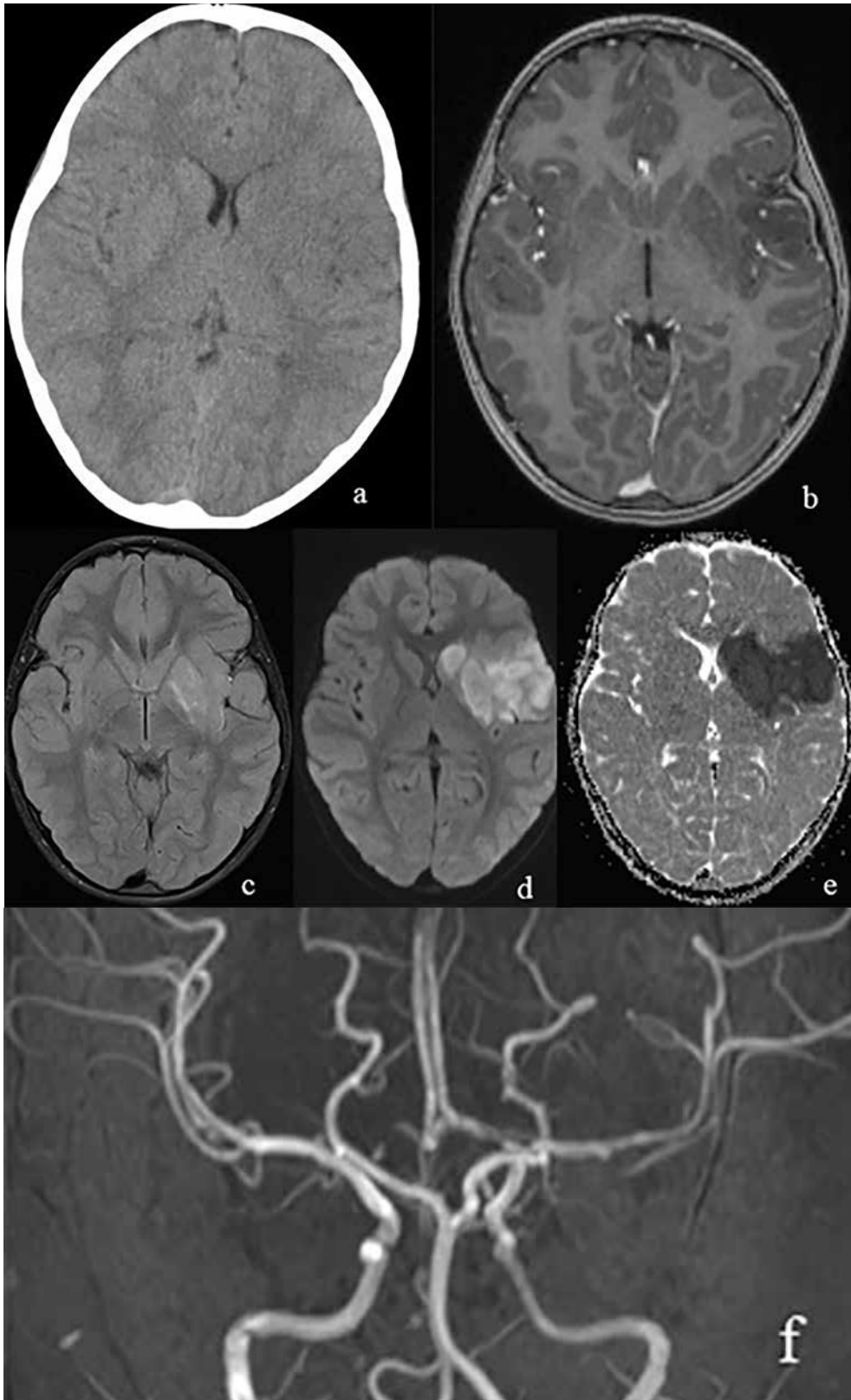


Figure 1. CT and MRI of an ischemic stroke in the left MCA (a - axial CT showing no features of stroke in the early stages; b-f MRI: b - T1W axial; c - T2W FLAIR axial; d - DW axial; e - ADC axial; f - TOF)

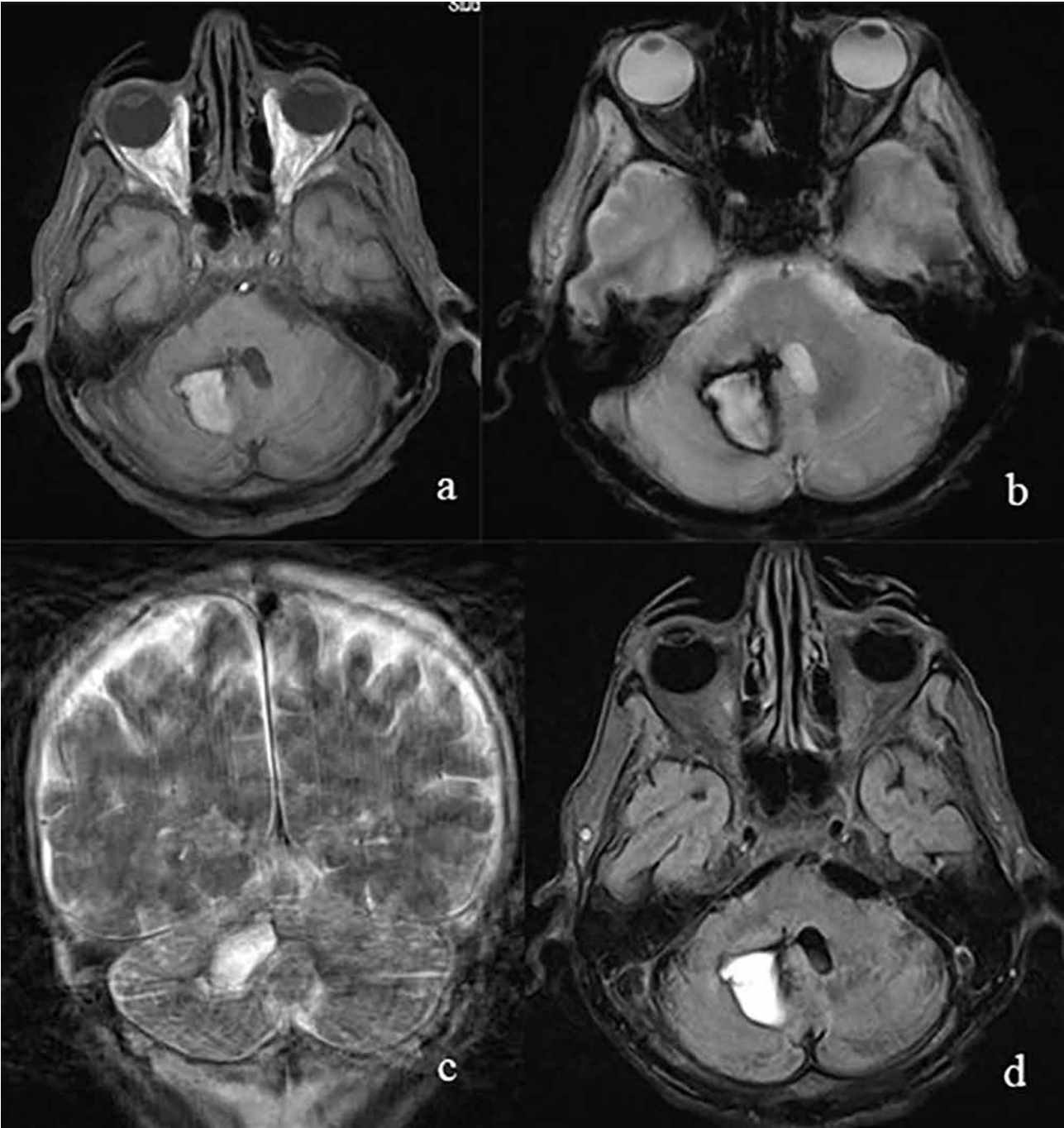


Figure 2. MRI of a non-traumatic haemorrhage at the right cerebellum hemisphere (a -T1W axial; b- T2W fl2d hemo axial; c- T2W coronal (movement artefacts); d- T2W FLAIR axial).

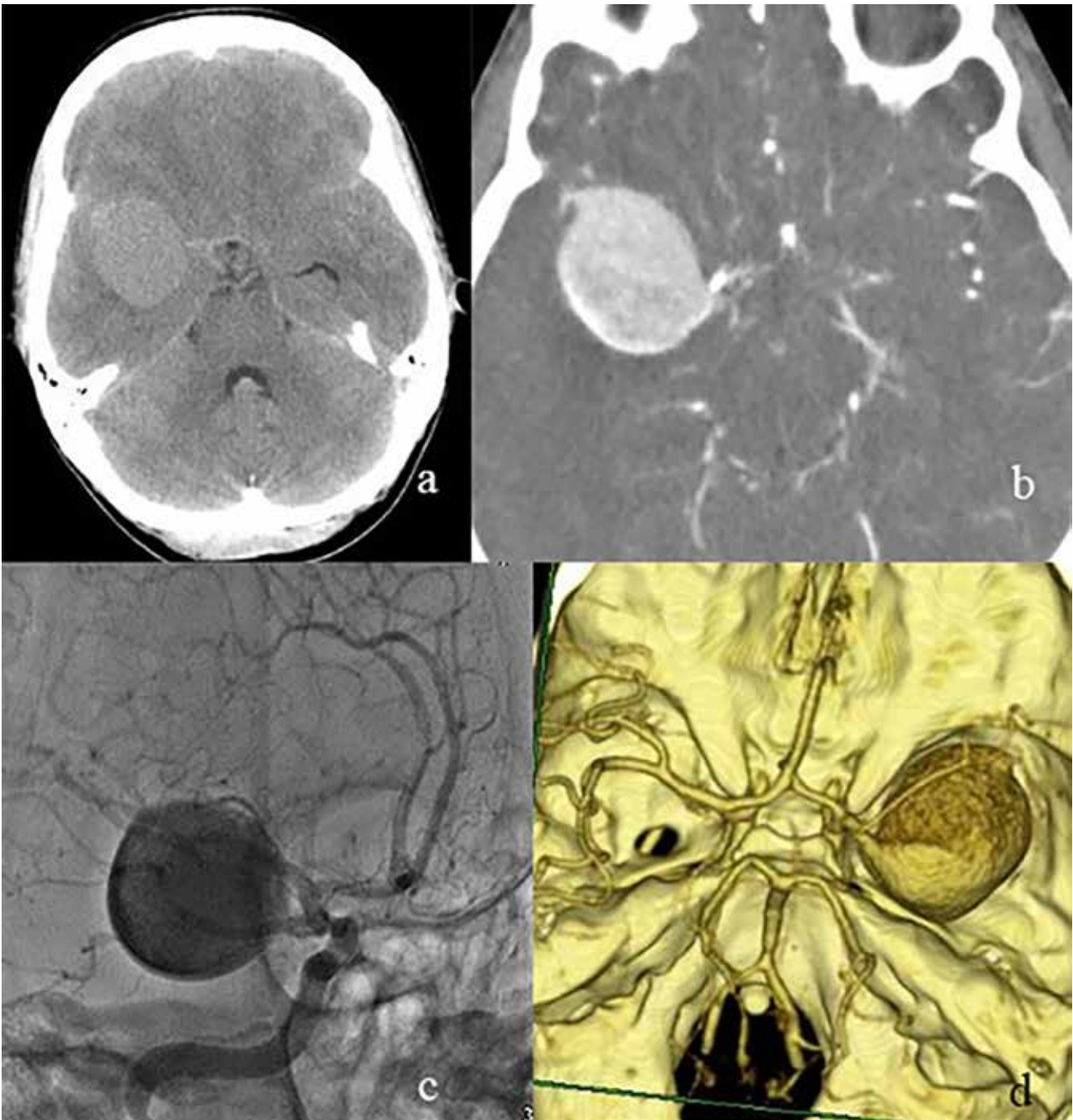


Figure 3. Saccular aneurysm at ACM dex. vessel: a - axial CT; b - CT angiography basic; c - angiography; d - CT angiography 3D reconstruction.

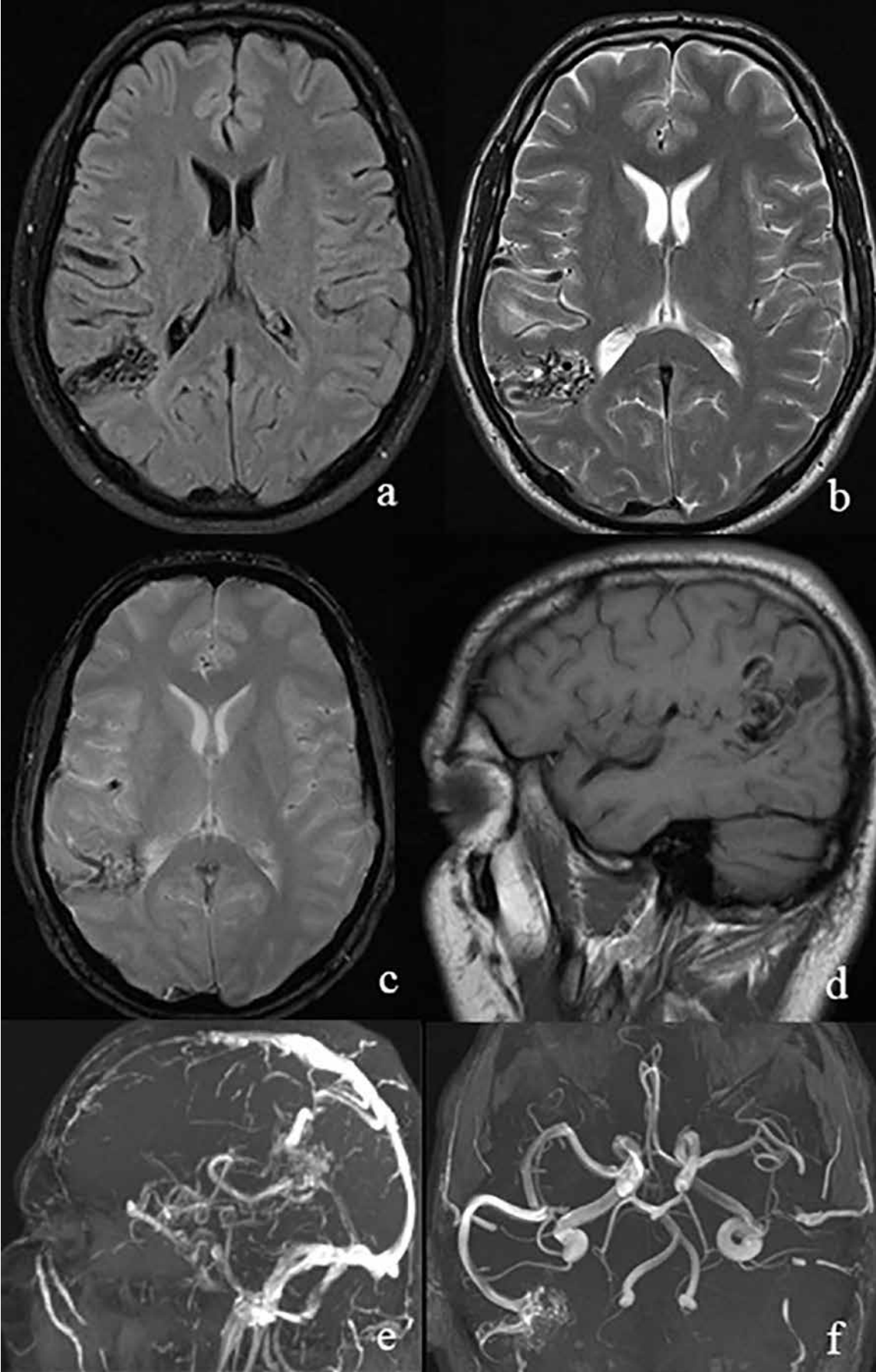


Figure 4. Arteriovenous malformation, MRI (a - T2W FLAIR axial; b - T2W axial; c - T2W f12d hemo axial; d - T1W sagittal; e - TOF vein; f - TOF arterial).

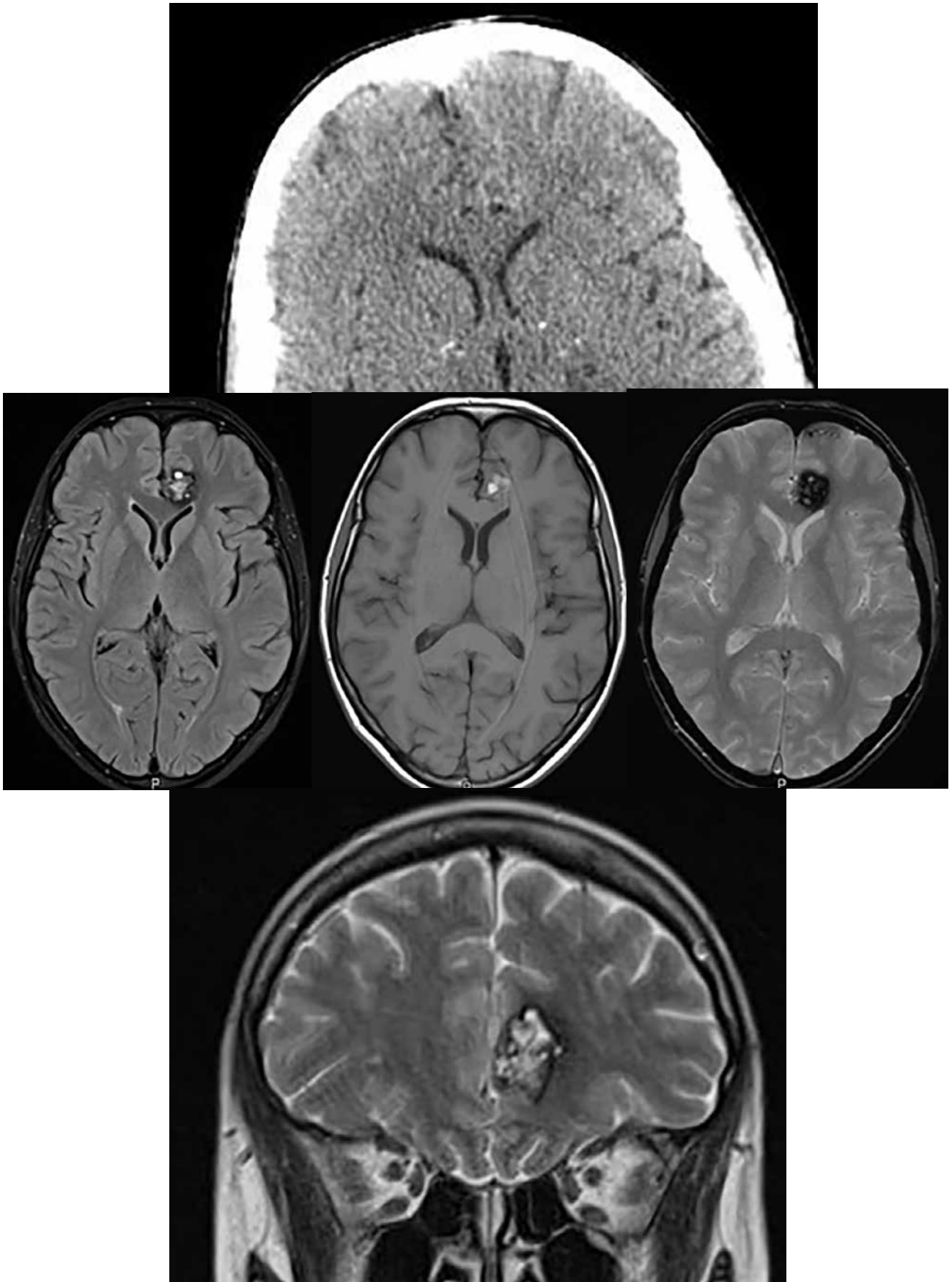


Figure 5. Cavernoma at the left frontal lobe (a - axial CT; MRI: b - T2W/FLAIR axial; c - T1W axial; d - T2W fl2 hemo axial; e - T2W coronal).

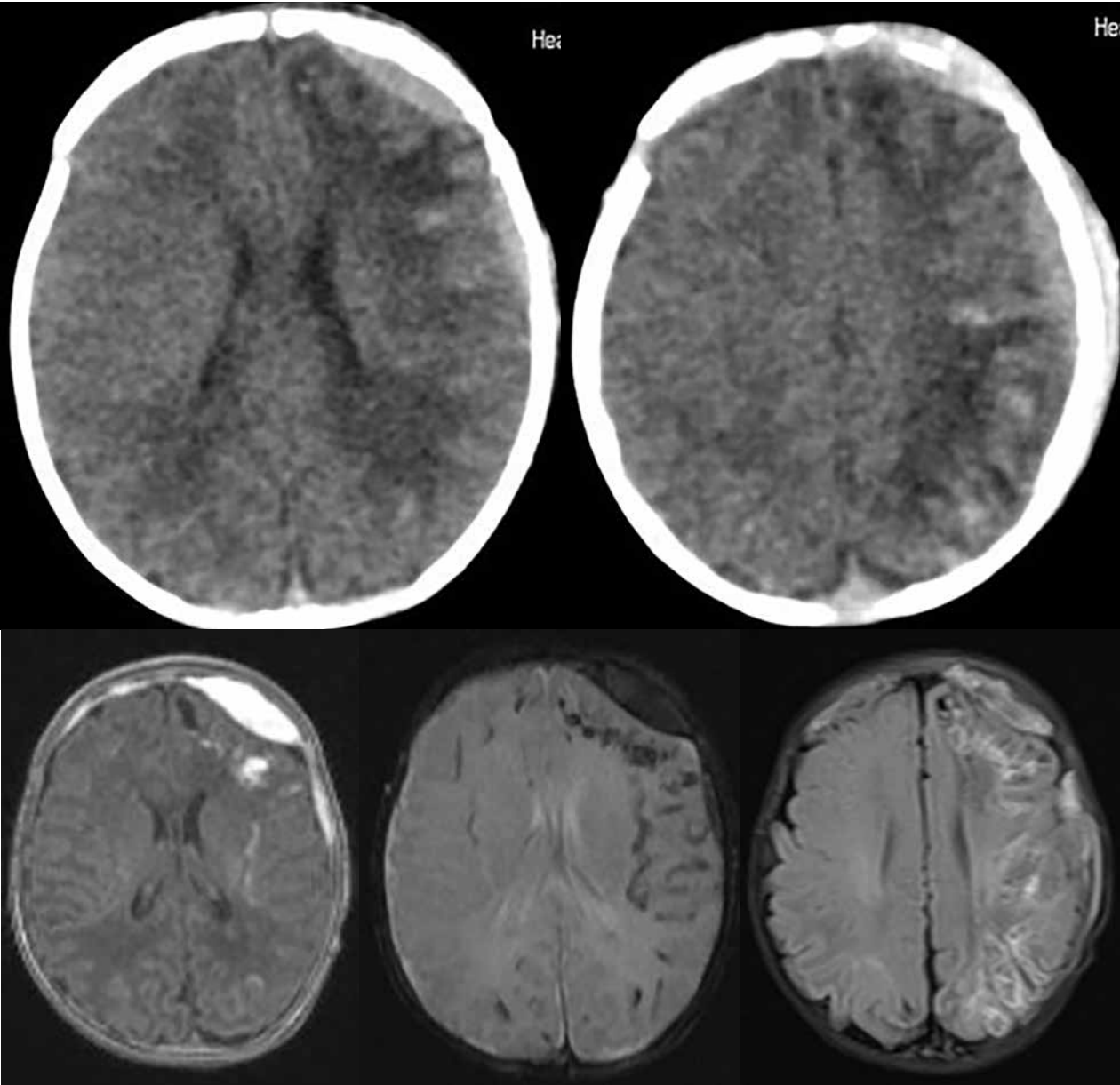


Figure 6. Sturge-Weber syndrome with an acute epidural haematoma at the left frontal lobe as a concomitant pathology (a, b – axial CT; axial MRI: c - T1W; d - T2W fl2d hemo; e - T2W FLAIR).

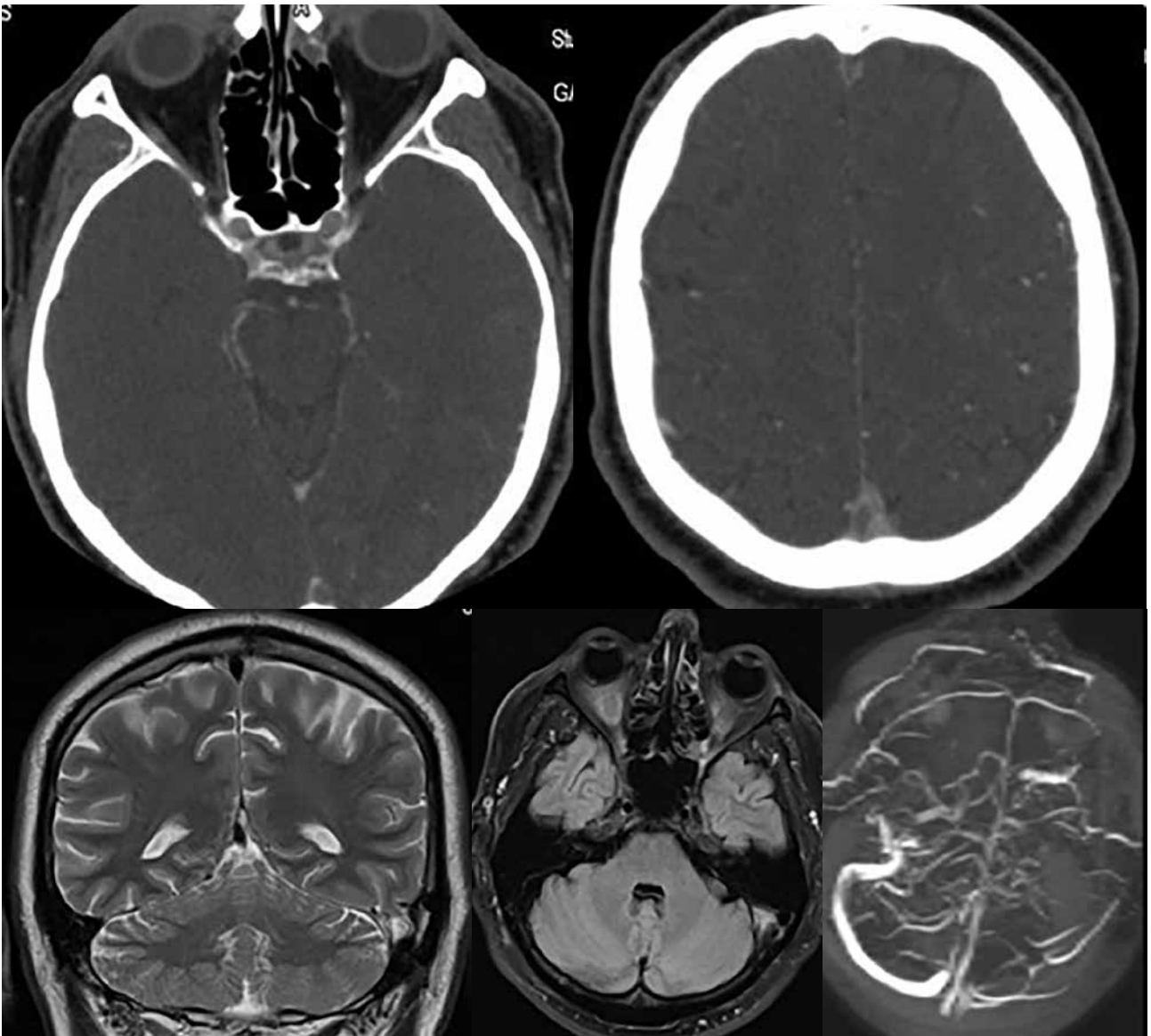


Figure 7. Multiple different venous sinus thromboses (thrombosis of the superior sagittal sinus: a, b - axial CT; and thrombosis of the left transversal sinus vein MRI: c - T2W coronal; d - T2W FLAIR axial; e - TOF).

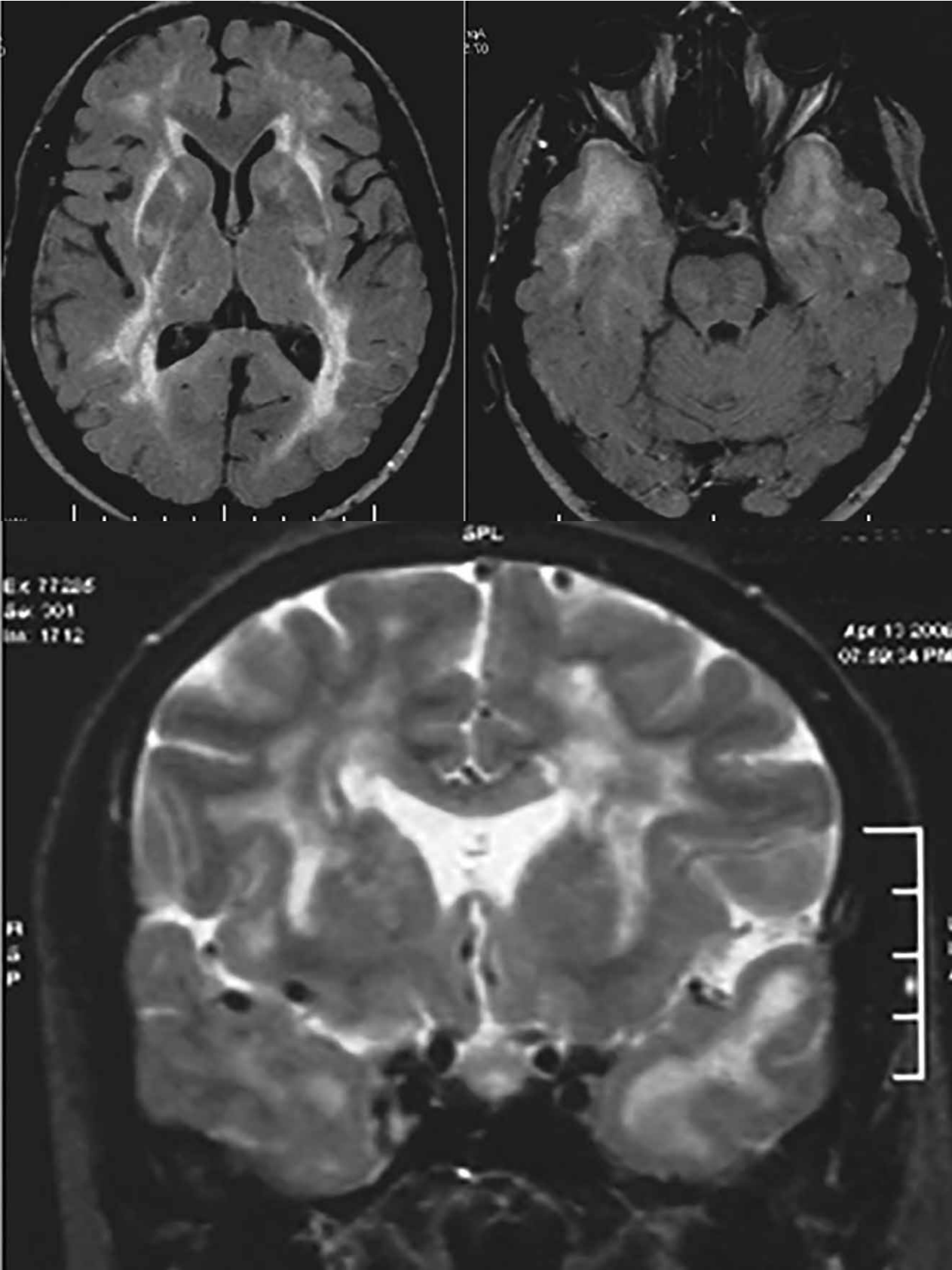


Figure 8. CADASIL, MRI (a, b - T2W FLAIR axial; c - T2W coronal).

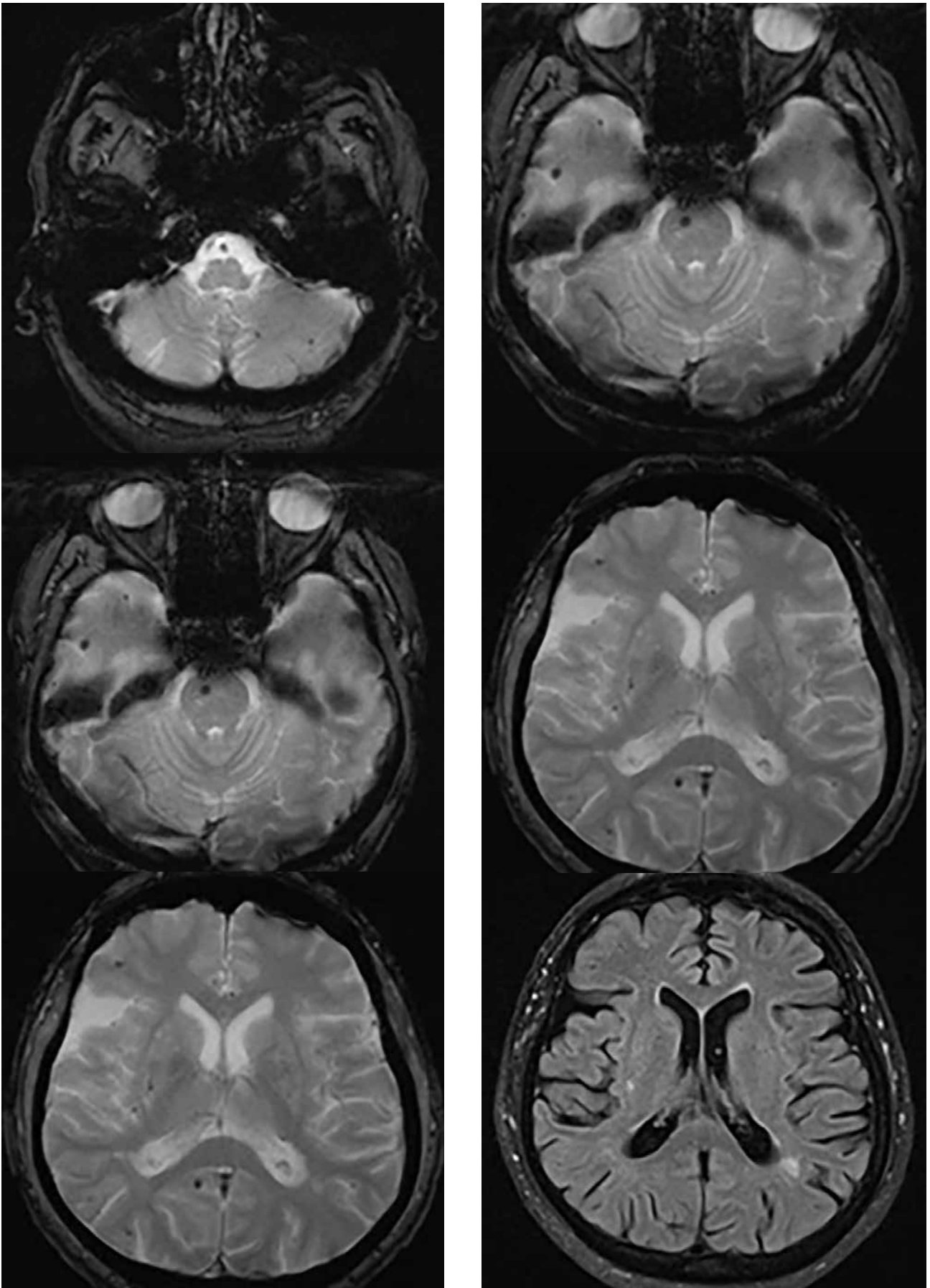


Figure 9. Cerebral amyloid angiopathy and encephalopathy, MRI (a - e T2W fl2d hemo axial; f - T2W/FLAIR axial).

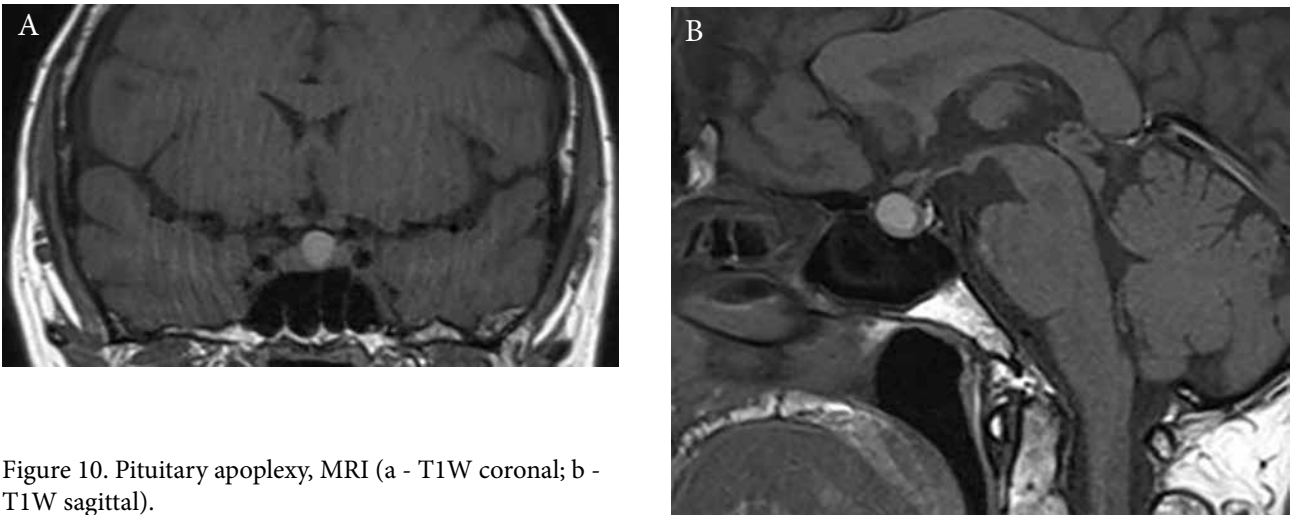


Figure 10. Pituitary apoplexy, MRI (a - T1W coronal; b - T1W sagittal).

CONCLUSIONS

Headaches attributed to cranial and cerebral vascular disorders vary in etiology, clinical and radiological manifestation. Therefore, a good understanding of the purpose that each imaging modality serves is required. CT imaging is a widely available and a quick diagnostic tool which, unfortunately, is also associated with ionizing radiation. MRI is a sensitive brain parenchymal lesion evaluation tool that does not expose patients to radiation and enables the evaluation of small pathological structures in different sequences. However, MRI scans take longer, are more expensive, and not as widely accessible as CT scanners. Other imaging modalities provide additional information on the intraluminal, metabolic, or perfusion changes in the brain when initial imaging is not sufficient and requires clarification.

REFERENCES

1. Paul Rizzoli WJM. Headache. *Am J Med.* 2017;325–46.
2. Stovner L, Hagen K, Jensen R, Katsarava Z, Lipton R, Scher A, et al. The Global Burden of Headache: A Documentation of Headache Prevalence and Disability Worldwide. *Cephalalgia.* 2007;27(3):193–210.
3. Goldstein J, Camargo C, Pelletier A, Edlow J. Headache in United States Emergency Departments. *Cephalalgia.* 2006;26(6):684–90.
4. Starling AJ. Diagnosis and Management of Headache in Older Adults [Internet]. Vol. 93, *Mayo Clinic Proceedings.* Elsevier; 2018. p. 252–62.
5. Newell KA. Headache Mistakes You Do Not Want to Make [Internet]. Vol. 2, *Physician Assistant Clinics.* Elsevier; 2017. p. 503–17.
6. Long BJ, Koyfman A. Benign Headache Management in the Emergency Department. *J Emerg Med.* 2018;54(4):458–68.
7. Sacco RL, Kasner SE, Broderick JP, Caplan LR, Connors JJ, Culebras A, et al. An updated definition of stroke for the 21st century: A statement for healthcare professionals from the American heart association/American stroke association. *Stroke.* 2013;44(7):2064–89.
8. Béjot Y, Bailly H, Durier J, Giroud M. Epidemiology of stroke in Europe and trends for the 21st century. *Press Medicale.* 2016;45(12):e391–8.
9. Pollak L, Shlomo N, Korn Lubetzki I. Headache in stroke according to National Acute Stroke Israeli Survey. *Acta Neurol Scand.* 2016;135(4):469–75.
10. Jamieson DG, Cheng NT, Skliut M. Headache and Acute Stroke. *Curr Pain Headache Rep.* 2014;18(9):444.
11. Lester MS, Liu BP. Imaging in the Evaluation of Headache. *Med Clin North Am.* 2013;97(2):243–65.
12. Hansen AP, Marcussen NS, Klit H, Andersen G, Finnerup NB, Jensen TS. Pain following stroke: A prospective study. *Eur J Pain (United Kingdom).* 2012;16(8):1128–36.
13. Harrison RA, Field TS. Post Stroke Pain: Identification, Assessment, and Therapy. *Cerebrovasc Dis.* 2015;39(3–4):190–201.
14. Cassella CR, Jagoda A. Ischemic Stroke: Advances in Diagnosis and Management [Internet]. Vol. 35, *Emergency Medicine Clinics of North America.* Elsevier; 2017. p. 911–30.
15. Powers WJ, Rabinstein AA, Ackerson T, Adeoye OM, Bambakidis NC, Becker K, et al. 2018 Guidelines for the Early Management of Patients With Acute Ischemic Stroke: A Guideline for Healthcare Professionals From the American Heart Association/American Stroke Association. *Stroke.* 2018;49(3):e46–99.
16. Vilela P, Rowley HA. Brain ischemia: CT and MRI techniques in acute ischemic stroke. *Eur J Radiol.* 2017;96:162–72.
17. Powers WJ, Derdeyn CP, Biller J, Coffey CS, Hoh BL, Jauch EC, et al. 2015 American Heart Association/American Stroke Association Focused Update of the 2013 Guidelines for the Early Management of Patients With Acute Ischemic Stroke Regarding Endovascular Treatment. *Stroke.* 2015;46(10):3020–35.
18. Wardlaw JM, Mielke O. Early Signs of Brain Infarction at CT: Observer Reliability and Outcome after Thrombolytic Treatment—Systematic Review. *Radiology.* 2005;235(2):444–53.
19. Schröder J, Thomalla G. A critical review of Alberta stroke program early CT score for evaluation of acute stroke imaging. *Front Neurol.* 2017;7:245.
20. Jauch EC, Saver JL, Adams HP, Bruno A, Connors JJ (Buddy), Demaerschalk BM, et al. Guidelines for the Early Management of Patients With Acute Ischemic Stroke. 2013;
21. Latchaw RE, Alberts MJ, Lev MH, Connors JJ, Harbaugh RE, Higashida RT, et al. Recommendations for Imaging of Acute Ischemic Stroke. *Stroke.* 2009;40(11):3646–78.
22. Wintermark M, Professor A, Sanelli P, Albers GW, Bello J, Derdeyn C, et al. Imaging Recommendations for Acute Stroke and Transient Ischemic Attack Patients: A Joint Statement by the American Society of Neuroradiology, the American College of Radiology and the Society of NeuroInterventional Surgery. *AJNR Am J Neuroradiol.* 2013;34(11):117–27.
23. González RG. Clinical MRI of acute ischemic stroke. *J Magn Reson Imaging.* 2012;36(2):259–71.
24. Lebedeva ER, Gurary NM, Olesen J. Headache in transient ischemic attacks. *J Headache Pain.* 2018;19(1):60.
25. Lee W, Frayne J. Transient ischaemic attack clinic: An evaluation of diagnoses and clinical decision making. *J Clin Neurosci.* 2015;22(4):645–8.
26. van Asch CJ, Luitse MJ, Rinkel GJ, van der Tweel I, Algra A, Klijn CJ. Incidence, case fatality, and functional outcome of intracerebral haemorrhage over time, according to age, sex, and ethnic origin: a systematic review and meta-analysis. *Lancet Neurol.* 2010;9(2):167–76.
27. Meretoja A, Strbian D, Putaala J, Curtze S, Haapaniemi E, Mustanoja S, et al. SMASH-U: A proposal for etiologic classification of intracerebral hemorrhage. *Stroke.* 2012;43(10):2592–7.
28. Koivunen R-J, Satopää J, Meretoja A, Strbian D, Haapaniemi E, Niemelä M, et al. Incidence, risk factors, etiology, severity and short-term outcome of non-traumatic intracerebral hemorrhage in young adults. *Eur J Neurol.* 2015;22(1):123–32.
29. Rothrock JF. Headaches caused by vascular disorders. *Neurol Clin.* 2014;32(2):305–19.
30. (IHS) HCC of the IHS. Headache Classification Committee of the International Headache Society (IHS) The International Classification of Headache Disorders, 3rd edition. *Cephalalgia.* 2018;38(1):1–211.
31. Alerhand S, Lay C. Spontaneous Intracerebral Hemorrhage. In: *Emergency Medicine Clinics of North America.* Elsevier; 2017. p. 825–45.
32. Chalela JA, Kidwell CS, Nentwich LM, Luby M, Butman JA, Demchuk AM, et al. Magnetic resonance imaging and computed tomography in emergency assessment of patients with suspected acute stroke: a prospective comparison. *Lancet.* 2007;369(9558):293–8.
33. Fiebach JB, Schellinger PD, Gass A, Kucinski T, Siebler M, Villringer A, et al. Stroke magnetic resonance imaging is accurate in hyperacute intracerebral hemorrhage: a multicenter study on the validity of stroke imaging. *Stroke.* 2004;35(2):502–6.
34. Safatli D, Günther A, Schlattmann P, Schwarz F, Kalff R, Ewald C. Predictors of 30-day mortality in patients with spontaneous primary intracerebral hemorrhage. *Surg Neurol Int.* 2016;7(19):510.
35. Wada R, Aviv RI, Fox AJ, Sahlas DJ, Gladstone DJ, Tomlinson G, et al. CT Angiography “Spot Sign” Predicts Hema-

- toma Expansion in Acute Intracerebral Hemorrhage. *Stroke*. 2007;38(4):1257–62.
36. Demchuk AM, Dowlatshahi D, Rodriguez-Luna D, Molina CA, Blas YS, Dzialowski I, et al. Prediction of haematoma growth and outcome in patients with intracerebral haemorrhage using the CT-angiography spot sign (PREDICT): a prospective observational study. *Lancet Neurol*. 2012;11(4):307–14.
37. Park SY, Kong MH, Kim JH, Kang DS, Song KY, Huh SK. Role of “Spot Sign” on CT Angiography to Predict Hematoma Expansion in Spontaneous Intracerebral Hemorrhage. *J Korean Neurosurg Soc*. 2010;48(5):399.
38. Martí-Fàbregas J, Delgado-Mederos R, Granell E, Morenas Rodríguez E, Marín Lahoz J, Dinia L, et al. Microbleed Burden and Hematoma Expansion in Acute Intracerebral Hemorrhage. *Eur Neurol*. 2013;70(3–4):175–8.
39. Hemphill JC, Greenberg SM, Anderson CS, Becker K, Bendok BR, Cushman M, et al. Guidelines for the Management of Spontaneous Intracerebral Hemorrhage: A Guideline for Healthcare Professionals from the American Heart Association/American Stroke Association. *Stroke*. 2015;46(7):2032–60.
40. Shoamanesh A, Catanese L, Sakai O, Pikula A, Kase CS. Diffusion-Weighted imaging hyperintensities in intracerebral hemorrhage: Microinfarcts or microbleeds? *Ann Neurol*. 2013;73(6):795–6.
41. Kamel H, Navi BB, Hemphill JC. A Rule to Identify Patients Who Require Magnetic Resonance Imaging After Intracerebral Hemorrhage. *Neurocrit Care*. 2013;18(1):59–63.
42. McCormack RF, Hutson A. Can Computed Tomography Angiography of the Brain Replace Lumbar Puncture in the Evaluation of Acute-onset Headache After a Negative Noncontrast Cranial Computed Tomography Scan? *Acad Emerg Med*. 2010;17(4):444–51.
43. Ashraf R, Akhtar M, Akhtar S, Manzoor I. Diagnostic accuracy of flair in detection of acute subarachnoid hemorrhage in patients presenting with severe headache. *Journal of Neuroradiology*. 2018;
44. Yesilaras M, Kilic TY, Yesilaras S, Atilla OD, Öncel D, Çamlar M. The diagnostic and prognostic value of the optic nerve sheath diameter on CT for diagnosis spontaneous subarachnoid hemorrhage. *Am J Emerg Med*. 2017;35(10):1408–13.
45. van Gijn J, Kerr RS, Rinkel GJ. Subarachnoid haemorrhage. *Lancet*. 2007;369(9558):306–18.
46. Tabatabai RR, Swadron SP. Headache in the Emergency Department: Avoiding Misdiagnosis of Dangerous Secondary Causes. *Emerg Med Clin North Am*. 2016;34(4):695–716.
47. Rogers A, Furyk J, Banks C, Chu K. Diagnosis of subarachnoid haemorrhage: A survey of Australasian emergency physicians and trainees. *Emerg Med Australas*. 2014;26(5):468–73.
48. Swadron SP. Pitfalls in the Management of Headache in the Emergency Department. *Emerg Med Clin North Am*. 2010;28(1):127–47.
49. Farzad A, Radin B, Oh JS, Teague HM, Euerle BD, Nable J V, et al. Emergency diagnosis of subarachnoid hemorrhage: An evidence-based debate [Internet]. Vol. 44, *Journal of Emergency Medicine*. 2013. p. 1045–53.
50. Bonita R, Thomson S. Subarachnoid hemorrhage: Epidemiology, diagnosis, management, and outcome. *Stroke*. 1985;16(4):591–4.
51. Byyny RL, Mower WR, Shum N, Gabayan GZ, Fang S, Baraff LJ. Sensitivity of Noncontrast Cranial Computed Tomography for the Emergency Department Diagnosis of Subarachnoid Hemorrhage. *Ann Emerg Med*. 2008;51(6):697–703.
52. Wiesmann M, Mayer TE, Yousry I, Medele R, Hamann GF, Brückmann H. Detection of hyperacute subarachnoid hemorrhage of the brain by using magnetic resonance imaging. *J Neurosurg*. 2002;96(4):684–9.
53. Mitchell P, Wilkinson ID, Hoggard N, Paley MN, Jellinek DA, Powell T, et al. Detection of subarachnoid haemorrhage with magnetic resonance imaging. *J Neurol Neurosurg Psychiatry*. 2001;70(2):205–11.
54. Graff-Radford J, Fugate JE, Klaas J, Flemming KD, Brown RD, Rabinstein AA. Distinguishing clinical and radiological features of non-traumatic convexal subarachnoid hemorrhage. *Eur J Neurol*. 2016;23(5):839–46.
55. Connolly ES, Rabinstein AA, Carhuapoma JR, Derdeyn CP, Dion J, Higashida RT, et al. Guidelines for the management of aneurysmal subarachnoid hemorrhage: A guideline for healthcare professionals from the american heart association/american stroke association [Internet]. Vol. 43, *Stroke*. 2012. p. 1711–37.
56. Wu X, Kalra VB, Forman HP, Malhotra A. Cost-effectiveness analysis of CTA and LP for evaluation of suspected SAH after negative non-contrast CT. *Clin Neurol Neurosurg*. 2016;142:104–11.
57. Edlow JA. What Are the Unintended Consequences of Changing the Diagnostic Paradigm for Subarachnoid Hemorrhage After Brain Computed Tomography to Computed Tomographic Angiography in Place of Lumbar Puncture? *Acad Emerg Med*. 2010;17(9):991–5.
58. Dubosh NM, Bellolio MF, Rabinstein AA, Edlow JA. Sensitivity of Early Brain Computed Tomography to Exclude Aneurysmal Subarachnoid Hemorrhage. *Stroke*. 2016;47(3):750–5.
59. Blok KM, Rinkel GJE, Majoie CBLM, Hendrikse J, Braaksma M, Tijssen CC, et al. CT within 6 hours of headache onset to rule out subarachnoid hemorrhage in nonacademic hospitals. *Neurology*. 2015;84(19):1927–32.
60. Perry JJ, Stiell IG, Sivilotti MLA, Bullard MJ, Émond M, Symington C, et al. Sensitivity of computed tomography performed within six hours of onset of headache for diagnosis of subarachnoid haemorrhage: Prospective cohort study. *BMJ*. 2011;343(7817):d4277.
61. Carpenter CR, Hussain AM, Ward MJ, Zipfel GJ, Fowler S, Pines JM, et al. Spontaneous Subarachnoid Hemorrhage: A Systematic Review and Meta-analysis Describing the Diagnostic Accuracy of History, Physical Examination, Imaging, and Lumbar Puncture With an Exploration of Test Thresholds. *Acad Emerg Med*. 2016;23(9):963–1003.
62. Migdal VL, Wu WK, Long D, McNaughton CD, Ward MJ, Self WH. Risk-benefit analysis of lumbar puncture to evaluate for nontraumatic subarachnoid hemorrhage in adult ED patients. *Am J Emerg Med*. 2015;33(11):1597–601.
63. Cooper JG, Smith B, Hassan TB. A retrospective review of sudden onset severe headache and subarachnoid haemorrhage on the clinical decision unit. *Eur J Emerg Med*. 2016;23(5):356–62.
64. Mark DG, Hung Y-Y, Offerman SR, Rauchwerger AS, Reed ME, Chettipally U, et al. Nontraumatic Subarachnoid Hemorrhage in the Setting of Negative Cranial Computed

- Tomography Results: External Validation of a Clinical and Imaging Prediction Rule. *Ann Emerg Med*. 2013;62(1):1–10.e1.
65. Mortimer AM, Bradley MD, Stoodley NG, Renowden SA. Thunderclap headache: Diagnostic considerations and neuroimaging features [Internet]. Vol. 68, *Clinical Radiology*. W.B. Saunders; 2013. p. e101–13.
66. Al-Mufti F, Mayer SA. Neurocritical Care of Acute Subdural Hemorrhage. *Neurosurg Clin N Am*. 2017;28(2):267–78.
67. Vega RA, Valadka AB. Natural History of Acute Subdural Hematoma. *Neurosurg Clin N Am*. 2017;28(2):247–55.
68. Avis SP. Nontraumatic Acute Subdural Hematoma: A Case Report and Review of the Literature. *Am J Forensic Med Pathol*. 1993;14(2):130–4.
69. Carroll JJ, Lavine SD, Meyers PM. Imaging of Subdural Hematomas. *Neurosurg Clin N Am*. 2017;28(2):179–203.
70. Gentry LR, Godersky JC, Thompson B, Dunn VD. Prospective comparative study of intermediate-field MR and CT in the evaluation of closed head trauma. *AJR Am J Roentgenol*. 1988;150(3):673–82.
71. Thapa A, KC B, Shakya B. Pure Acute-on-Chronic Subdural Hematoma Due to Ruptured Posterior Communicating Artery Aneurysm: Unsuspecting Entity. *World Neurosurg*. 2018;114:335–8.
72. Verhey LH, Wang W, Adel JG. True Cortical Saccular Aneurysm Presenting as an Acute Subdural Hematoma. *World Neurosurg*. 2018;113:58–61.
73. Mathais Q, Esnault P, Dagain A, Sellier A, Simon PY, Prunet B, et al. Spontaneous pure subacute subdural haematoma without subarachnoid haemorrhage caused by rupture of middle cerebral artery aneurysm. *Anaesth Crit Care Pain Med*. 2018;37(6):623–4.
74. Koerbel A, Ernemann U, Freudenstein D. Acute subdural haematoma without subarachnoid haemorrhage caused by rupture of an internal carotid artery bifurcation aneurysm: Case report and review of literature. *Br J Radiol*. 2005;78(931):646–50.
75. Awaji K, Inokuchi R, Ikeda R, Haisa T. Nontraumatic Pure Acute Subdural Hematoma Caused by a Ruptured Cortical Middle Cerebral Artery Aneurysm: Case Report and Literature Review [Internet]. Vol. 3, *NMC Case Report Journal*. 2016. p. 63–6.
76. Inokuchi G, Makino Y, Yajima D, Motomura A, Chiba F, Torimitsu S, et al. A case of acute subdural hematoma due to ruptured aneurysm detected by postmortem angiography. *Int J Legal Med*. 2016;130(2):441–6.
77. Brisman JL, Song JK, Newell DW. Cerebral Aneurysms. *N Engl J Med*. 2006;355(9):928–39.
78. Brown RD, Broderick JP. Unruptured intracranial aneurysms: epidemiology, natural history, management options, and familial screening. *Lancet Neurol*. 2014;13(4):393–404.
79. Schwartz RB, Tice HM, Hooten SM, Hsu L, Stieg PE. Evaluation of cerebral aneurysms with helical CT: correlation with conventional angiography and MR angiography. *Radiology*. 1994;192(3):717–22.
80. Hacin-Bey L, Provenzale JM. Current imaging assessment and treatment of intracranial aneurysms. *Am J Roentgenol*. 2011;196:32–44.
81. Pradilla G, Wicks RT, Hadelsberg U, Gailloud P, Coon AL, Huang J, et al. Accuracy of computed tomography angiography in the diagnosis of intracranial aneurysms. *World Neurosurg*. 2013;80(6):845–52.
82. Li M-H, Li Y-D, Tan H-Q, Gu B-X, Chen Y-C, Wang W, et al. Contrast-free MRA at 3.0 T for the detection of intracranial aneurysms. *Neurology*. 2011;77(7):667–76.
83. Sailer AMH, Wagemans BAJM, Nelemans PJ, De Graaf R, Van Zwam WH. Diagnosing intracranial aneurysms with mr angiography : Systematic review and meta-analysis. *Stroke*. 2014;45(1):119–26.
84. Stafa A, Leonardi M. Role of Neuroradiology in Evaluating Cerebral Aneurysms. *Interv Neuroradiol*. 2008;14:23–37.
85. Dalton A, Dobson G, Prasad M, Mukerji N. De novo intracerebral arteriovenous malformations and a review of the theories of their formation. *Br J Neurosurg*. 2018;32(3):305–11.
86. Mohr JP, Kejda-Scharler J, Pile-Spellman J. Diagnosis and treatment of arteriovenous malformations topical collection on stroke. *Curr Neurol Neurosci Rep*. 2013;13(2):324.
87. Lang S-S, Beslow LA, Bailey RL, Vossough A, Ekstrom J, Heuer GG, et al. Follow-up imaging to detect recurrence of surgically treated pediatric arteriovenous malformations. *J Neurosurg Pediatr*. 2012;9(5):497–504.
88. Saleh RS, Singhal A, Lohan D, Duckwiler G, Finn P, Ruehm S. Assessment of cerebral arteriovenous malformations with high temporal and spatial resolution contrast-enhanced magnetic resonance angiography: A review from protocol to clinical application [Internet]. Vol. 19, *Topics in Magnetic Resonance Imaging*. 2008. p. 251–7.
89. Serulle Y, Miller TR, Gandhi D. Dural Arteriovenous Fistulae: Imaging and Management [Internet]. Vol. 26, *Neuroimaging Clinics of North America*. 2016. p. 247–58.
90. Elhammady MS, Ambekar S, Heros RC. Epidemiology, clinical presentation, diagnostic evaluation, and prognosis of cerebral dural arteriovenous fistulas. In: *Handbook of Clinical Neurology*. 2017. p. 99–105.
91. Srinivasan VM, Chintalapani G, Duckworth EAM, Kan P. Application of 4-Dimensional Digital Subtraction Angiography for Dural Arteriovenous Fistulas. *World Neurosurg*. 2016;96:24–30.
92. Tsai L-K, Liu H-M, Jeng J-S. Diagnosis and management of intracranial dural arteriovenous fistulas. *Expert Rev Neurother*. 2016;16(3):307–18.
93. Naserrudin NS, Mohammad Raffiq MA. Dural arteriovenous fistula mimicking temporal arteritis. *Clin Neurol Neurosurg*. 2019;176:44–6.
94. Stapleton CJ, Barker FG. Cranial Cavernous Malformations. *Stroke*. 2018;49(4):1029–35.
95. Daniele Rigamonti, M.D., Mark N. Hadley, M.D., Burton P. Drayer, M.D., Peter C. Johnson, M.D., M.A., Karen Hoenig-Rigamonti, M.D., J. Thomas Knight, M.D., and Robert F. Spetzler MD. Cerebral cavernous malformations. *N Engl J Med*. 1998;319(6):343–7.
96. Comi AM. Sturge-Weber syndrome. *Handb Clin Neurol*. 2015;132:157–68.
97. Higueros E, Roe E, Granell E, Baselga E. Síndrome de Sturge-Weber: revisión [Internet]. Vol. 108, *Actas Dermo-Sifilograficas*. Elsevier; 2017. p. 407–17.
98. Sudarsanam A, Ardern-Holmes SL. Sturge-Weber syndrome: From the past to the present [Internet]. Vol. 18, *European Journal of Paediatric Neurology*. W.B. Saunders; 2014. p. 257–66.

99. Pinto AL, Chen L, Friedman R, Grant PE, Poduri A, Takeoka M, et al. Sturge-Weber Syndrome: Brain Magnetic Resonance Imaging and Neuropathology Findings. *Pediatr Neurol*. 2016;58:25–30.
100. Koster MJ, Matteson EL, Warrington KJ. Large-vessel giant cell arteritis: Diagnosis, monitoring and management [Internet]. Vol. 57, *Rheumatology (United Kingdom)*. 2018. p. ii32–ii42.
101. Christoph BT, Gregor S, Markus A, Daniel S, Christof R, Thomas D. The clinical benefit of imaging in the diagnosis and treatment of giant cell arteritis [Internet]. Vol. 148, *Swiss Medical Weekly*. EMH Media; 2018.
102. Neshet G. The diagnosis and classification of giant cell arteritis. *J Autoimmun*. 2014;48–49:73–5.
103. Hyeon Jeong Cho, MS, Justin Bloomberg, DO, Jeffrey Nichols M. Giant Cell Arteritis. *Disease-a-month*. 2017;367–87.
104. Buttgerief F, Dejaco C, Matteson EL, Dasgupta B. Polymyalgia Rheumatica and Giant Cell Arteritis. *JAMA*. 2016;315(22):2442–58.
105. Jem Ninan, Susan Lester CH. Giant Cell Arteritis. *Best Pract Res Clin Rheumatol*. 2016;367–87.
106. Frohman L, Wong ABC, Matheos K, Leon-Alvarado LG, Danesh-Meyer H V. New developments in giant cell arteritis. *Surv Ophthalmol*. 2016;61(4):400–21.
107. Mandal J, Chung SA. Primary Angiitis of the Central Nervous System [Internet]. Vol. 43, *Rheumatic Disease Clinics of North America*. Elsevier; 2017. p. 503–18.
108. Salvarani C, Brown RD, Calamia KT, Christianson TJH, Weigand SD, Miller D V, et al. Primary central nervous system vasculitis: analysis of 101 patients. *Ann Neurol*. 2007;62(5):442–51.
109. Rodriguez-Pla A, Monach PA. Primary Angiitis of the Central Nervous System in Adults and Children. *Rheum Dis Clin North Am*. 2015;41(1):47–62.
110. Hajj-Ali RA, Calabrese LH. Primary angiitis of the central nervous system. *Autoimmun Rev*. 2013;12(4):463–6.
111. Boulouis G, De Boysson H, Zuber M, Guillevin L, Meary E, Costalat V, et al. Primary Angiitis of the Central Nervous System: Magnetic Resonance Imaging Spectrum of Parenchymal, Meningeal, and Vascular Lesions at Baseline. *Stroke*. 2017;48(5):1248–55.
112. Singhal AB, Topcuoglu MA, Fok JW, Kursun O, Nogueira RG, Frosch MP, et al. Reversible cerebral vasoconstriction syndromes and primary angiitis of the central nervous system: clinical, imaging, and angiographic comparison. *Ann Neurol*. 2016;79(6):882–94.
113. Gan C, Maingard J, Giles L, Phal PM, Tan KM. Primary angiitis of the central nervous system presenting as a mass lesion. *J Clin Neurosci*. 2015;22(9):1528–31.
114. Engelter ST, Traenka C, Von Hessling A, Lyrer PA. Diagnosis and treatment of cervical artery dissection. *Neurol Clin*. 2015;33(2):421–41.
115. Kim Y-K, Schulman S. Cervical artery dissection: Pathology, epidemiology and management. *Thromb Res*. 2009;123(6):810–21.
116. Robertson JJ, Koefman A. Cervical Artery Dissections: A Review. *J Emerg Med*. 2016;51(5):508–18.
117. Mattioni A, Paciaroni M, Sarchielli P, Murasecco D, Pelliccioli GP, Calabresi P. Multiple cranial nerve palsies in a patient with internal carotid artery dissection. *Eur Neurol*. 2007;58(2):125–7.
118. Dittrich R, Ritter MA, Ringelstein EB. Ultrasound in spontaneous cervical artery dissection. *Perspect Med*. 2012;1–12:250–4.
119. Kim YK, Schulman S. Cervical artery dissection: Pathology, epidemiology and management [Internet]. Vol. 123, *Thrombosis Research*. Pergamon; 2009. p. 810–21.
120. Debette S, Leys D. Cervical-artery dissections: predisposing factors, diagnosis, and outcome. *Lancet Neurol*. 2009;8(7):668–78.
121. Provenzale JM, Sarikaya B. Comparison of test performance characteristics of MRI, MR angiography, and CT angiography in the diagnosis of carotid and vertebral artery dissection: A review of the medical literature [Internet]. Vol. 193, *American Journal of Roentgenology*. 2009. p. 1167–74.
122. Hanning U, Sporns PB, Schmiedel M, Ringelstein EB, Heindel W, Wiendl H, et al. CT versus MR Techniques in the Detection of Cervical Artery Dissection. *J Neuroimaging*. 2017;27(6):607–12.
123. Thomas MA, Pearce WH, Rodriguez HE, Helenowski IB, Eskandari MK. Durability of Stroke Prevention with Carotid Endarterectomy and Carotid Stenting. *Surgery*. 2018;164(6):1271–8.
124. Galyfos G, Sianou A, Filis K. Cerebral hyperperfusion syndrome and intracranial hemorrhage after carotid endarterectomy or carotid stenting: A meta-analysis. *J Neurol Sci*. 2017;381:74–82.
125. Kirchoff-Torres KF, Bakradze E. Cerebral Hyperperfusion Syndrome After Carotid Revascularization and Acute Ischemic Stroke. *Curr Pain Headache Rep*. 2018;22(4):24.
126. Doepp F, Kebelmann-Betzling C, Kivi A, Schreiber SJ. Stenosis or Hyperperfusion in Sickle Cell Disease - Ultrasound Assessment of Cerebral Blood Flow Volume. *Ultrasound Med Biol*. 2012;38(8):1333–8.
127. Van Mook WNKA, Rennenberg RJMW, Schurink GW, Van Oostenbrugge RJ, Mess WH, Hofman PAM, et al. Cerebral hyperperfusion syndrome. *Lancet Neurol*. 2005;4(12):877–88.
128. Zhang Y, Kumar A, Tezel JB, Zhou Y. Imaging Evidence for Cerebral Hyperperfusion Syndrome after Intravenous Tissue Plasminogen Activator for Acute Ischemic Stroke. *Case Rep Neurol Med*. 2016;2016:1–5.
129. Yoo DH, Roh HG, Choi SS, Moon J, Lee J, Cho YD, et al. Staged carotid artery stenting in patients with severe carotid stenosis: Multicenter experience. *J Clin Neurosci*. 2018;53:74–8.
130. Ferro JM, Canhão P, Stam J, Bousser MG, Barinagarrementeria F. Prognosis of Cerebral Vein and Dural Sinus Thrombosis: Results of the International Study on Cerebral Vein and Dural Sinus Thrombosis (ISCVT). *Stroke*. 2004;35(3):664–70.
131. Coutinho JM, Zuurbier SM, Aramideh M, Stam J. The incidence of cerebral venous thrombosis: A cross-sectional study. *Stroke*. 2012;43(12):3375–7.
132. Coutinho JM. Cerebral venous thrombosis. *J Thromb Haemost*. 2015;13:S238–44.
133. Rizzo L, Crasto SG, Rudà R, Gallo G, Tola E, Garaballo D, et al. Cerebral venous thrombosis: role of CT, MRI and MRA in the emergency setting. *Radiol Med*. 2010;115(2):313–25.
134. Saposnik G, Barinagarrementeria F, Brown RD, Bushnell CD, Cucchiara B, Cushman M, et al. Diagnosis and manage-

- ment of cerebral venous thrombosis: A statement for healthcare professionals from the American Heart Association/American Stroke Association. *Stroke*. 2011;42(4):1158–92.
135. Rodallec MH, Krainik A, Feydy A, Hélias A, Colombani J-M, Jullès M-C, et al. Cerebral Venous Thrombosis and Multidetector CT Angiography: Tips and Tricks. *RadioGraphics*. 2006;26(suppl_1):S5–18.
 136. Buyck P-J, De Keyzer F, Vanneste D, Wilms G, Thijs V, Demaerel P. CT Density Measurement and H:H Ratio Are Useful in Diagnosing Acute Cerebral Venous Sinus Thrombosis. *Am J Neuroradiol*. 2013;34(8):1568–72.
 137. Goldberg AL, Rosenbaum AE, Wang H, Kim WS, Lewis VL, Hanley DF. Computed tomography of dural sinus thrombosis. *J Comput Assist Tomogr*. 1986;10(1):16–20.
 138. Long B, Koyfman A, Runyon MS. Cerebral Venous Thrombosis: A Challenging Neurologic Diagnosis. *Emerg Med Clin North Am*. 2017;35(4):869–78.
 139. Leach JL, Fortuna RB, Jones B V., Gaskill-Shipley MF. Imaging of Cerebral Venous Thrombosis: Current Techniques, Spectrum of Findings, and Diagnostic Pitfalls. *RadioGraphics*. 2006;26(suppl_1):S19–41.
 140. Gratama van Andel HA, van Boven LJ, van Walderveen MA, Venema HW, van Rijn JC, Stam J, et al. Interobserver variability in the detection of cerebral venous thrombosis using CT venography with matched mask bone elimination. *Clin Neurol Neurosurg*. 2009;111(9):717–23.
 141. Ozsvath RR, Casey SO, Lustrin ES, Alberico RA, Hassankhani A, Patel M. Cerebral Venography: Comparison of CT and MR Projection Venography. *Am J Roentgenol*. 1997;169(6):699–707.
 142. Ayanzen RH, Bird CR, Keller PJ, McCully FJ, Theobald MR, Heiserman JE. Cerebral MR venography: Normal anatomy and potential diagnostic pitfalls. *Am J Neuroradiol*. 2000;21(1):74–8.
 143. Boukobza M, Crassard I, Bousser MG, Chabriat H. MR imaging features of isolated cortical vein thrombosis: Diagnosis and follow-up. *Am J Neuroradiol*. 2009;30(2):344–8.
 144. Farb RI, Scott JN, Willinsky RA, Montanera WJ, Wright GA, TerBrugge KG. Intracranial Venous System: Gadolinium-enhanced Three-dimensional MR Venography with Auto-triggered Elliptic Centric-ordered Sequence—Initial Experience. *Radiology*. 2003;226(1):203–9.
 145. Silvis SM, de Sousa DA, Ferro JM, Coutinho JM. Cerebral venous thrombosis. *Nat Rev Neurol*. 2017;13(9):555–65.
 146. Dinkin MJ, Patsalides A. Venous Sinus Stenting for Idiopathic Intracranial Hypertension: Where Are We Now? *Neurol Clin*. 2017;35(1):59–81.
 147. Ducros A. Reversible cerebral vasoconstriction syndrome. *Lancet Neurol*. 2012;11(10):906–17.
 148. Ducros A, Wolff V. The Typical Thunderclap Headache of Reversible Cerebral Vasoconstriction Syndrome and its Various Triggers. *Headache J Head Face Pain*. 2016;56(4):657–73.
 149. Ducros A, Boukobza M, Porcher R, Sarov M, Valade D, Bousser M-G. The clinical and radiological spectrum of reversible cerebral vasoconstriction syndrome. A prospective series of 67 patients. *Brain*. 2007;130(12):3091–101.
 150. Singhal AB, Hajj-Ali RA, Topcuoglu MA, Fok J, Bena J, Yang D, et al. Reversible Cerebral Vasoconstriction Syndromes. *Arch Neurol*. 2011;68(8):1005–12.
 151. Wolff V, Ducros A. Reversible Cerebral Vasoconstriction Syndrome Without Typical Thunderclap Headache. *Headache J Head Face Pain*. 2016;56(4):674–87.
 152. Wolff V, Armspach J-P, Lauer V, Rouyer O, Ducros A, Marescaux C, et al. Ischaemic Strokes with Reversible Vasoconstriction and without Thunderclap Headache: A Variant of the Reversible Cerebral Vasoconstriction Syndrome? *Cerebrovasc Dis*. 2015;39(1):31–8.
 153. Katz BS, Fugate JE, Ameriso SF, Pujol-Lereis VA, Mandrekar J, Flemming KD, et al. Clinical Worsening in Reversible Cerebral Vasoconstriction Syndrome. *JAMA Neurol*. 2014;71(1):68–73.
 154. Marder CP, Donohue MM, Weinstein JR, Fink KR. Multimodal imaging of reversible cerebral vasoconstriction syndrome: A series of 6 cases. *Am J Neuroradiol*. 2012;33(7):1403–10.
 155. Miller TR, Shivashankar R, Mossa-Basha M, Gandhi D. Reversible Cerebral Vasoconstriction Syndrome, Part 2: Diagnostic Work-Up, Imaging Evaluation, and Differential Diagnosis. *Am J Neuroradiol*. 2015;36(9):1580–8.
 156. Kumar S, Goddeau RP, Selim DMH, Thomas PA, Schlaug G, Alhazzani PA, et al. Atraumatic convexal subarachnoid hemorrhage Clinical presentation, imaging patterns, and etiologies. *Neurology*. 2010;74(11):893–9.
 157. Lin C-H, Chen Y-Y, Chiu L-A, Lee K-W. Dual energy computed tomography angiography for the rapid diagnosis of reversible cerebral vasoconstriction syndromes: report of a case. *Acta Neurol Taiwan*. 2013;22(1):36–42.
 158. Kameda T, Namekawa M, Shimazaki H, Minakata D, Matsuura T, Nakano I. Unique combination of hyperintense vessel sign on initial FLAIR and delayed vasoconstriction on MRA in reversible cerebral vasoconstriction syndrome: A case report. *Cephalalgia*. 2014;34(13):1093–6.
 159. Chen S-P, Fuh J-L, Lirng J-F, Wang S-J. Hyperintense vessels on flair imaging in reversible cerebral vasoconstriction syndrome. *Cephalalgia*. 2012;32(4):271–8.
 160. Chen S-P, Fuh J-L, Wang S-J, Chang F-C, Lirng J-F, Fang Y-C, et al. Magnetic resonance angiography in reversible cerebral vasoconstriction syndromes. *Ann Neurol*. 2010;67(5):648–56.
 161. Chen S-P, Fuh J-L, Chang F-C, Lirng J-F, Shia B-C, Wang S-J. Transcranial color doppler study for reversible cerebral vasoconstriction syndromes. *Ann Neurol*. 2008;63(6):751–7.
 162. Ducros A, Bousser M-G. Reversible cerebral vasoconstriction syndrome. *Pract Neurol*. 2009;9(5):256–67.
 163. Mandell DM, Matouk CC, Farb RI, Krings T, Agid R, terBrugge K, et al. Vessel Wall MRI to Differentiate Between Reversible Cerebral Vasoconstriction Syndrome and Central Nervous System Vasculitis. *Stroke*. 2012;43(3):860–2.
 164. Obusez EC, Hui F, Hajj-ali RA, Cerejo R, Calabrese LH, Hammad T, et al. High-Resolution MRI Vessel Wall Imaging: Spatial and Temporal Patterns of Reversible Cerebral Vasoconstriction Syndrome and Central Nervous System Vasculitis. *Am J Neuroradiol*. 2014;35(8):1527–32.
 165. Komatsu T, Kimura T, Yagishita A, Takahashi K, Koide R. A case of reversible cerebral vasoconstriction syndrome presenting with recurrent neurological deficits: Evaluation using noninvasive arterial spin labeling MRI. *Clin Neurol Neurosurg*. 2014;126:96–8.
 166. Rosenbloom MH, Singhal AB. CT Angiography and Diffusion-Perfusion MR Imaging in a Patient with Ipsilateral Reversible Cerebral Vasoconstriction after Carotid Endarterectomy. *Am J Neuroradiol*. 2007;28(5):920–2.

167. Zhao WY, Krings T, Alvarez H, Ozanne A, Holmin S, Lasjaunias P. Management of spontaneous haemorrhagic intracranial vertebrobasilar dissection: review of 21 consecutive cases. *Acta Neurochir (Wien)*. 2007;149(6):585–96; discussion 596.
168. Santos-Franco JA, Zenteno M, Lee A. Dissecting aneurysms of the vertebrobasilar system. A comprehensive review on natural history and treatment options. *Neurosurg Rev*. 2008;31(2):131–40.
169. Metso A, Metso T, Salonen O, Tatlisumak T. Response to Letter by Arnold et al. *Stroke*. 2007;38(11):141.
170. Debette S, Compter A, Labeyrie M-A, Uyttenboogaart M, Metso TM, Majersik JJ, et al. Epidemiology, pathophysiology, diagnosis, and management of intracranial artery dissection. *Lancet Neurol*. 2015;14(6):640–54.
171. Wang Y, Lou X, Li Y, Sui B, Sun S, Li C, et al. Imaging investigation of intracranial arterial dissecting aneurysms by using 3 T high-resolution MRI and DSA: from the interventional neuroradiologists' view. *Acta Neurochir (Wien)*. 2014;156(3):515–25.
172. Mizutani T. Natural course of intracranial arterial dissections. *J Neurosurg*. 2011;114(4):1037–44.
173. Ahn SS, Kim BM, Suh SH, Kim DJ, Kim DI, Shin YS, et al. Spontaneous Symptomatic Intracranial Vertebrobasilar Dissection: Initial and Follow-up Imaging Findings. *Radiology*. 2012;264(1):196–202.
174. Kilarski LL, Rutten-Jacobs LCA, Bevan S, Baker R, Hassan A, Hughes DA, et al. Prevalence of CADASIL and fabry disease in a cohort of MRI defined younger onset Lacunar Stroke. *Kaya N*, editor. *PLoS One*. 2015;10(8):e0136352.
175. Moreton FC, Razvi SSM, Davidson R, Muir KW. Changing clinical patterns and increasing prevalence in CADASIL. *Acta Neurol Scand*. 2014;130(3):197–203.
176. Razvi SSM, Davidson R, Bone I, Muir K. The prevalence of cerebral autosomal dominant arteriopathy with subcortical infarcts and leukoencephalopathy (CADASIL) in the west of Scotland. *J Neurol Neurosurg Psychiatry*. 2005;76(5):739–41.
177. Narayan SK, Gorman G, Kalaria RN, Ford GA, Chinnery PF. The minimum prevalence of CADASIL in northeast England. *Neurology*. 2012;78(13):1025–7.
178. Kilarski LL, Rutten-Jacobs LCA, Bevan S, Baker R, Hassan A, Hughes DA, et al. Prevalence of CADASIL and fabry disease in a cohort of MRI defined younger onset Lacunar Stroke. *Kaya N*, editor. *PLoS One*. 2015;10(8):e0136352.
179. Chabriat H, Joutel A, Dichgans M, Tournier-Lasserre E, Bousser M-G. CADASIL. *Lancet Neurol*. 2009;8(7):643–53.
180. Stromillo ML, Dotti MT, Battaglini M, Mortilla M, Bianchi S, Plewnia K, et al. Structural and metabolic brain abnormalities in preclinical cerebral autosomal dominant arteriopathy with subcortical infarcts and leukoencephalopathy. *J Neurol Neurosurg Psychiatry*. 2009;80(1):41–7.
181. Zhu S, Nahas SJ. CADASIL: Imaging Characteristics and Clinical Correlation. *Curr Pain Headache Rep*. 2016;20(10):57.
182. Auer DP, Pütz B, Gössl C, Elbel G-K, Gasser T, Dichgans M. Differential Lesion Patterns in CADASIL and Sporadic Subcortical Arteriosclerotic Encephalopathy: MR Imaging Study with Statistical Parametric Group Comparison. *Radiology*. 2001;218(2):443–51.
183. Di Donato I, Bianchi S, De Stefano N, Dichgans M, Dotti MT, Duering M, et al. Cerebral Autosomal Dominant Arteriopathy with Subcortical Infarcts and Leukoencephalopathy (CADASIL) as a model of small vessel disease: update on clinical, diagnostic, and management aspects. *BMC Med*. 2017;15(1):41.
184. Singhal S, Rich P, Markus HS. The spatial distribution of MR imaging abnormalities in cerebral autosomal dominant arteriopathy with subcortical infarcts and leukoencephalopathy and their relationship to age and clinical features. *Am J Neuroradiol*. 2005;26(10):2481–7.
185. Coulthard A, Blank SC, Bushby K, Kalaria RN, Burn DJ. Distribution of cranial MRI abnormalities in patients with symptomatic and subclinical CADASIL. *Br J Radiol*. 2000;73(867):256–65.
186. Pavlakis SG, Phillips PC, DiMauro S, De Vivo DC, Rowland LP. Mitochondrial myopathy, encephalopathy, lactic acidosis, and stroke-like episodes: A distinctive clinical syndrome. *Ann Neurol*. 1984;16(4):481–8.
187. Hirano M, Ricci E, Koenigsberger MR, Defendini R, Pavlakis SG, DeVivo DC, et al. Melas: an original case and clinical criteria for diagnosis. *Neuromuscul Disord*. 1992;2(2):125–35.
188. Malhotra K, Liebeskind DS. Imaging of MELAS. *Curr Pain Headache Rep*. 2016;20(9):54.
189. Ito H, Mori K, Kagami S. Neuroimaging of stroke-like episodes in MELAS. *Brain Dev*. 2011;33(4):283–8.
190. Walecka A. CT and MRI imaging of the brain in MELAS syndrome. *Polish J Radiol*. 2013;78(3):61–5.
191. Pauli W, Zarzycki A, Krzyształowski A, Walecka A. CT and MRI imaging of the brain in MELAS syndrome. *Polish J Radiol*. 2013;78(3):61–5.
192. Kim IO, Kim JH, Kim WS, Hwang YS, Yeon KM, Han MC. Mitochondrial myopathy-encephalopathy-lactic acidosis-and stroke-like episodes (MELAS) syndrome: CT and MR findings in seven children. *AJR Am J Roentgenol*. 1996;166(3):641–5.
193. Schaefer PW, Buonanno FS, Gonzalez RG, Schwamm LH. Diffusion-weighted imaging discriminates between cytotoxic and vasogenic edema in a patient with eclampsia. *Stroke*. 1997;28(5):1082–5.
194. Kim JH, Lim MK, Jeon TY, Rha JH, Eo H, Yoo SY, et al. Diffusion and perfusion characteristics of MELAS (mitochondrial myopathy, encephalopathy, lactic acidosis, and stroke-like episode) in thirteen patients. *Korean J Radiol*. 2011;12(1):15–24.
195. Yonemura K, Hasegawa Y, Kimura K, Minematsu K, Yamaguchi T. Diffusion-weighted MR imaging in a case of mitochondrial myopathy, encephalopathy, lactic acidosis, and stroke-like episodes. *AJNR Am J Neuroradiol*. 2001;22(2):269–72.
196. Abe K, Yoshimura H, Tanaka H, Fujita N, Hikita T, Sakoda S. Comparison of conventional and diffusion-weighted MRI and proton MR spectroscopy in patients with mitochondrial encephalomyopathy, lactic acidosis, and stroke-like events. *Neuroradiology*. 2004;46(2):113–7.
197. Ito H, Mori K, Harada M, Minato M, Naito E, Takeuchi M, et al. Serial brain imaging analysis of stroke-like episodes in MELAS. *Brain Dev*. 2008;30(7):483–8.
198. Tzoulis C, Bindoff LA. Serial Diffusion Imaging in a Case of Mitochondrial Encephalomyopathy, Lactic Acidosis, and Stroke-Like Episodes. *Stroke*. 2009;40(2):e15–7.
199. Koga Y, Akita Y, Nishioka J, Yatsuga S, Povalko N, Tanabe Y, et al. L-Arginine improves the symptoms of stroke-like epi-

- sodes in MELAS. *Neurology*. 2005;64(4):710–2.
200. Nishioka J, Akita Y, Yatsuga S, Katayama K, Matsuishi T, Ishibashi M, et al. Inappropriate intracranial hemodynamics in the natural course of MELAS. *Brain Dev*. 2008;30(2):100–5.
201. Yeh H-L, Chen Y-K, Chen W-H, Wang H-C, Chiu H-C, Lien L-M, et al. Perfusion status of the stroke-like lesion at the hyperacute stage in MELAS. *Brain Dev*. 2013;35(2):158–64.
202. Ikawa M, Okazawa H, Arakawa K, Kudo T, Kimura H, Fujibayashi Y, et al. PET imaging of redox and energy states in stroke-like episodes of MELAS. *Mitochondrion*. 2009;9(2):144–8.
203. Ikawa M, Yoneda M, Muramatsu T, Matsunaga A, Tsujikawa T, Yamamoto T, et al. Detection of preclinically latent hyperperfusion due to stroke-like episodes by arterial spin-labeling perfusion MRI in MELAS patients. *Mitochondrion*. 2013;13(6):676–80.
204. Xie S. MR OEF Imaging in MELAS. *Methods Enzymol*. 2014;547:433–44.
205. Kamada K, Takeuchi F, Houkin K, Kitagawa M, Kuriaki S, Ogata A, et al. Reversible brain dysfunction in MELAS: MEG, and (1)H MRS analysis. *J Neurol Neurosurg Psychiatry*. 2001;70(5):675–8.
206. Kodaka R, Itagaki Y, Matsumoto M, Nagai T, Okada S. A transcranial doppler ultrasonography study of cerebrovascular CO₂ reactivity in mitochondrial encephalomyopathy. *Stroke*. 1996;27(8):1350–3.
207. Suzuki J, Kodama N. Moyamoya disease--a review. *Stroke*. 1983;14(1):104–9.
208. Baba T, Houkin K, Kuroda S. Novel epidemiological features of moyamoya disease. *J Neurol Neurosurg Psychiatry*. 2008;79(8):900–4.
209. Xie A, Luo L, Ding Y, Li G. Ischemic and hemorrhagic moyamoya disease in adults: CT findings. *Int J Clin Exp Med*. 2015;8(11):21351–7.
210. Takahashi M, Miyauchi T, Kowada M. Computed tomography of Moyamoya disease: demonstration of occluded arteries and collateral vessels as important diagnostic signs. *Radiology*. 1980;134(3):671–6.
211. Kim J-M, Lee S-H, Roh J-K. Changing ischaemic lesion patterns in adult moyamoya disease. *J Neurol Neurosurg Psychiatry*. 2009;80(1):36–40.
212. Fujimura M, Bang OY, Kim JS. Moyamoya disease. *Front Neurol Neurosci*. 2016;40:204–20.
213. Yamada I, Matsushima Y, Suzuki S. Moyamoya disease: diagnosis with three-dimensional time-of-flight MR angiography. *Radiology*. 1992;184(3):773–8.
214. Brady AP, Stack JP, Ennis JT. Moyamoya disease--imaging with magnetic resonance. *Clin Radiol*. 1990;42(2):138–41.
215. Yamada I, Suzuki S, Matsushima Y. Moyamoya disease: comparison of assessment with MR angiography and MR imaging versus conventional angiography. *Radiology*. 1995;196(1):211–8.
216. Ohta T, Tanaka H, Kuroiwa T. Diffuse leptomeningeal enhancement, "ivy sign," in magnetic resonance images of moyamoya disease in childhood: case report. *Neurosurgery*. 1995;37(5):1009–12.
217. Le-Bao Yu L-B, Zhang Q, Shi Z-Y, Wang M-Q, Zhang D. High-resolution Magnetic Resonance Imaging of Moyamoya Disease. *Chin Med J (Engl)*. 2015;128(23):3231.
218. Yuan M, Liu Z, Wang Z, Li B, Xu L, Xiao X. High-resolution MR imaging of the arterial wall in moyamoya disease. *Neurosci Lett*. 2015;584:77–82.
219. Ryoo S, Cha J, Kim SJ, Choi JW, Ki C-S, Kim KH, et al. High-Resolution Magnetic Resonance Wall Imaging Findings of Moyamoya Disease. *Stroke*. 2014;45(8):2457–60.
220. Kim YJ, Lee DH, Kwon JY, Kang DW, Suh DC, Kim JS, et al. High resolution MRI difference between moyamoya disease and intracranial atherosclerosis. *Eur J Neurol*. 2013;20(9):1311–8.
221. Rafay MF, Armstrong D, Dirks P, MacGregor DL, deVeber G. Patterns of cerebral ischemia in children with moyamoya. *Pediatr Neurol*. 2015;52(1):65–72.
222. Kuroda S, Kashiwazaki D, Ishikawa T, Nakayama N, Houkin K. Incidence, Locations, and Longitudinal Course of Silent Microbleeds in Moyamoya Disease. *Stroke*. 2013;44(2):516–8.
223. Kikuta K, Takagi Y, Nozaki K, Sawamoto N, Fukuyama H, Hashimoto N. The presence of multiple microbleeds as a predictor of subsequent cerebral hemorrhage in patients with moyamoya disease. *Neurosurgery*. 2008;62(1):104–11.
224. Suzuki J, Takaku A. Cerebrovascular “Moyamoya” Disease. *Arch Neurol*. 1969;20(3):288.
225. Sasagawa A, Mikami T, Hirano T, Akiyama Y, Mikuni N. Characteristics of cerebral hemodynamics assessed by CT perfusion in moyamoya disease. *J Clin Neurosci*. 2018;47:183–9.
226. Toscano M, Puledda F, Viganò A, Vicenzini E, Guidetti G, Lenzi GL, et al. Hemodynamic features of non-aneurysmal subarachnoid hemorrhage in a case of familial moyamoya disease: a transcranial Doppler ultrasound study. *Eur Neurol*. 2014;72(5–6):330–2.
227. Lee W-J, Jung K-H, Lee K-J, Kim J-M, Lee S-T, Chu K, et al. Sonographic findings associated with stenosis progression and vascular complications in moyamoya disease. *J Neurosurg*. 2016;125(3):689–97.
228. Hara S, Tanaka Y, Ueda Y, Hayashi S, Inaji M, Ishiwata K, et al. Noninvasive Evaluation of CBF and Perfusion Delay of Moyamoya Disease Using Arterial Spin-Labeling MRI with Multiple Postlabeling Delays: Comparison with ¹⁵O-Gas PET and DSC-MRI. *Am J Neuroradiol*. 2017;38(4):696–702.
229. Kuhn FP, Warnock G, Schweingruber T, Sommerauer M, Buck A, Khan N. Quantitative H₂[15O]-PET in Pediatric Moyamoya Disease: Evaluating Perfusion before and after Cerebral Revascularization. *J Stroke Cerebrovasc Dis*. 2015;24(5):965–71.
230. Lee M, Zaharchuk G, Guzman R, Achrol A, Bell-Stephens T, Steinberg GK. Quantitative hemodynamic studies in moyamoya disease. *Neurosurg Focus*. 2009;26(4):E5.
231. Pantoni L. Cerebral small vessel disease: from pathogenesis and clinical characteristics to therapeutic challenges. *Lancet Neurol*. 2010;9(7):689–701.
232. Keage HA, Carare RO, Friedland RP, Ince PG, Love S, Nicoll JA, et al. Population studies of sporadic cerebral amyloid angiopathy and dementia: a systematic review. *BMC Neurol*. 2009;9(1):3.
233. Gorelick PB, Scuteri A, Black SE, DeCarli C, Greenberg SM, Iadecola C, et al. Vascular Contributions to Cognitive Impairment and Dementia. *Stroke*. 2011;42(9):2672–713.
234. Rosand J, Muzikansky A, Kumar A, Wisco JJ, Smith EE, Betensky RA, et al. Spatial clustering of hemorrhages in probable cerebral amyloid angiopathy. *Ann Neurol*. 2005;58(3):459–62.

235. Wilson D, Charidimou A, Werring DJ. Advances in understanding spontaneous intracerebral hemorrhage: insights from neuroimaging. *Expert Rev Neurother*. 2014;14(6):661–78.
236. Wilson D, Hostettler IC, Ambler G, Banerjee G, Jäger HR, Werring DJ. Convexity subarachnoid haemorrhage has a high risk of intracerebral haemorrhage in suspected cerebral amyloid angiopathy. *J Neurol*. 2017;264(4):664–73.
237. Greenberg SM, Vernooij MW, Cordonnier C, Viswanathan A, Al-Shahi R, Salman E, et al. Cerebral Microbleeds: A Field Guide to their Detection and Interpretation. *Lancet Neurol*. 2009;8(2):165–74.
238. Charidimou A, Werring DJ. Cerebral microbleeds: detection, mechanisms and clinical challenges. 2011;6(5):587–611.
239. Maxwell SS, Jackson CA, Paternoster L, Cordonnier C, Thijs V, Salman RA-S, et al. Genetic associations with brain microbleeds: Systematic review and meta-analyses. *Neurology*. 2011;77(2):158–67.
240. van Rooden S, van der Grond J, van den Boom R, Haan J, Linn J, Greenberg SM, et al. Descriptive Analysis of the Boston Criteria Applied to a Dutch-Type Cerebral Amyloid Angiopathy Population. *Stroke*. 2009;40(9):3022–7.
241. Greenberg SM, Eng JA, Ning M, Smith EE, Rosand J. Hemorrhage Burden Predicts Recurrent Intracerebral Hemorrhage After Lobar Hemorrhage. *Stroke*. 2004;35(6):1415–20.
242. Akoudad S, Portegies MLP, Koudstaal PJ, Hofman A, van der Lugt A, Ikram MA, et al. Cerebral Microbleeds Are Associated With an Increased Risk of Stroke. *Circulation*. 2015;132(6):509–16.
243. Charidimou A, Boulouis G, Haley K, Auriel E, Etten ES van, Fotiadis P, et al. White matter hyperintensity patterns in cerebral amyloid angiopathy and hypertensive arteriopathy. *Neurology*. 2016;86(6):505–11.
244. Linn J, Halpin A, Demaerel P, Ruhland J, Giese AD, Dichgans M, et al. Prevalence of superficial siderosis in patients with cerebral amyloid angiopathy. *Neurology*. 2010;74(17):1346–50.
245. Vernooij MW, Lugt A van der, Ikram MA, Wielopolski PA, Niessen WJ, Hofman A, et al. Prevalence and risk factors of cerebral microbleeds. *Neurology*. 2008;70(14):1208–14.
246. Roongpiboonsopit D, Charidimou A, William CM, Lauer A, Falcone GJ, Martinez-Ramirez S, et al. Cortical superficial siderosis predicts early recurrent lobar hemorrhage. *Neurology*. 2016;87(18):1863–70.
247. Charidimou A, Farid K, Baron J-C. Amyloid-PET in sporadic cerebral amyloid angiopathy. *Neurology*. 2017;89(14):1490–8.
248. Stam AH, Kothari PH, Shaikh A, Gschwendter A, Jen JC, Hodgkinson S, et al. Retinal vasculopathy with cerebral leukoencephalopathy and systemic manifestations. *Brain*. 2016;139(11):2909–22.
249. Pelzer N, Hoogeveen ES, Haan J, Bunnik R, Poot CC, van Zwet EW, et al. Systemic features of retinal vasculopathy with cerebral leukoencephalopathy and systemic manifestations: a monogenic small vessel disease. *J Intern Med*. 2018;
250. Glezer A, Bronstein MD, Glezer A, Bronstein MD. Pituitary apoplexy: pathophysiology, diagnosis and management. *Arch Endocrinol Metab*. 2015;59(3):259–64.
251. Fernandez A, Karavitaki N, Wass JAH. Prevalence of pituitary adenomas: a community-based, cross-sectional study in Banbury (Oxfordshire, UK). *Clin Endocrinol (Oxf)*. 2010;72(3):377–82.
252. Briet C, Salenave S, Bonneville J-F, Laws ER, Chanson P. Pituitary Apoplexy. *Endocr Rev*. 2015;36(6):622–45.
253. Randeve HS, Schoebel J, Byrne J, Esiri M, Adams CBT, Wass JAH. Classical pituitary apoplexy: clinical features, management and outcome. *Clin Endocrinol (Oxf)*. 1999;51(2):181–8.
254. Piotin M, Tampieri D, Rüfenacht DA, Mohr G, Garant M, Del Carpio R, et al. The various MRI patterns of pituitary apoplexy. *Eur Radiol*. 1999;9(5):918–23.
255. Laidlaw JD, Tress B, Gonzales MF, Wray AC, Ng WH, O'Brien JM. Coexistence of aneurysmal subarachnoid haemorrhage and pituitary apoplexy: Case report and review of the literature. *J Clin Neurosci*. 2014;10(4):478–82.
256. Sibal L, Ball SG, Connolly V, James RA, Kane P, Kelly WF, et al. Pituitary Apoplexy: A Review of Clinical Presentation, Management and Outcome in 45 Cases. *Pituitary*. 2004;7(3):157–63.
257. Gruber A, Clayton J, Kumar S, Robertson I, Howlett TA, Mansell P. Pituitary apoplexy: retrospective review of 30 patients—is surgical intervention always necessary? *Br J Neurosurg*. 2006;20(6):379–85.
258. Flanagan EP, Leep Hunderfund A, Giannini C, Meissner I. Addition of magnetic resonance imaging to computed tomography and sensitivity to blood in pituitary apoplexy. *Arch Neurol*. 2011;68(10):1336–7.
259. Semple PL, Jane JA, Lopes MBS, Laws ER. Pituitary apoplexy: correlation between magnetic resonance imaging and histopathological results. *J Neurosurg*. 2008;108(5):909–15.
260. Dubuisson AS, Beckers A, Stevenaert A. Classical pituitary tumour apoplexy: Clinical features, management and outcomes in a series of 24 patients. *Clin Neurol Neurosurg*. 2007;109(1):63–70.
261. Tosaka M, Sato N, Hirato J, Fujimaki H, Yamaguchi R, Kohga H, et al. Assessment of hemorrhage in pituitary macroadenoma by T2*-weighted gradient-echo MR imaging. *Am J Neuroradiol*. 2007;28(10):2023–9.